PEOPLE'S DEMOCRATIC REPUBLIC OF ALGERIA

MINISTRY OF HIGHER EDUCATION AND SCIENTIFIC RESEARCH

IBN-KHALDOUN UNIVERSITY OF TIARET

FACULTY OF APPLIED SCIENCE

DEPARTMENT OF MECHANICAL ENGINEERING

END OF STUDY MEMOIR

To obtain the Master's degree

Domain: Science and Technology

Mechanical Engineering

Specialty: Energetic

THESIS

Numerical Simulation of Abrasive Water Jet for Different Taper Inlet Angles

Submitted by:

MECHERI Fatima Zohra ;

ABID warda

Last name and first names	Grade	Exercise place	Qualité
Sahli Ahmed	Prof	UIK Tiaret	President
ABOUSHIGHIBA Hicham	MAA	UIK Tiaret	Examiner 1
KARAS Abdelkader	MCA	UIK Tiaret	supervisor
GOUICHICHE Madjid	MCB	UIK Tiaret	Guest
ABED Asma	PHD	UIK Tiaret	Guest

University year : 2016/2017

RÉPUBLIQUE ALGÉRIENNE DÉMOCRATIQUE ET POPULAIRE

MINISTÈRE DE L'ENSEIGNEMENT SUPÉRIEUR ET DE LA RECHERCHE SCIENTIFIQUE

UNIVERSITÉ IBN-KHALDOUN DE TIARET

FACULTÉ DES SCIENCES APPLIQUEES

DÉPARTEMENT DE GENIE MECANIQUE

MEMOIRE DE FIN D'ETUDES

Pour l'obtention du diplôme de Master

Domaine : Sciences et Technologie

Filière : Génie Mécanique

Spécialité: Energétique

THÈME

Simulation numérique du jet d'eau abrasive pour un angle d'entrée conique différent

Préparé par:

MECHERI Fatima Zohra

ABID Warda

Devant le Jury :

Nom et prénoms	Grade	Lieu d'exercice	Qualité
BOUZIDANE Ahmed	Prof	UIK Tiaret	Président
ABOUSHIGHIBA Hicham	MAA	UIK Tiaret	Examinateur 1
KARAS Abdelkader	MCA	UIK Tiaret	Encadreur
GOUICHICHE Madjid	MCB	UIK Tiaret	Invité
ABED Asma	PHD	UIK Tiaret	Invité

Année universitaire : 2016/2017

Dedicate

Thank you Allah (my God) for giving me the ability to write and reflect, the strength to believe, the patience to go to the end of the dream

and the happiness of lifting my hands to heaven and saying "Ya Kayoum"

I dedicate this modest work to the one who gave me life, the symbol of tenderness,

who sacrificed for my happiness and my success, to my mother ...

to my father, school of my childhood, which was my shadow during all the years of studies.

and who has been vigilant throughout my life in encouraging me to give me help and to protect myself.

To my adorable Islam and Rimasse

To my brothers and sisters

To all my friends without exception and my roommate,

I love you all, to all who are dear to me

To all those who love me.

Mecheri Fatima

Dedicate

With all my love, I dedicate my dissertation work to my dad Mhammed and my mother Fatima Belhabib who provide me in all my study years, with their patient, advices and praying for me.

A special feeling of gratitude to my loving husband DEBAGH Mohammed, who gives me the hope and supported me during my university days.

To my gorgeous sister Amina and her daughter Nadjla, my little sister Ihsan, my brother Djamal-Eddinne with my best wishes for them.

I also dedicate this dissertation to Aicha Hamdi, and her daughters Fatima, and Zohra DEBAGH. A special thanks to my uncle Nadjem Belhabib, and his son Ahmed Yassin.

To my little cousins Fathi, Mohammed Siradj, Ghofrane, Aicha

For my best friends: Karima, Assia, Shaima, Zaineb, Siham,

ABID WARDA

Acknowledgement

Firstly, we would like to thank Allah for being with us all the way of our lives thanks Allah.

We are indebted to our supervisor ***DR A. KARAS***, master of conference at university IBN KHALDOUN, who has been a constant source of encouragement, for his guidance during our research, his support, patient and inspiring suggestions.

Thanks to all the teachers that tough us during the two years of our master program.

We would also like to thank all the members that work in the IBN-Khaldoun University and especially to the workers in mechanical department.

A special thanks to our family that were a great support to us

Our greatest goes to our friends, we would never forget all the chats and beautiful moments we shared with some of our friends and classmates they were fundamental in supporting us during the stressful and difficult moment,

Also special thanks to all our classmates that studied with us in ***KSAR CHELALA***.

Lastly, we are very grateful to all the people

That we have met along the way of our study and our research.

Abstract:

A computational fluid dynamics (CFD) method has been developed to find out the particle and air, water velocity at the exit of the focus tube, the study has been carried out using a multi-phase approach, the abrasive particle were treated as a solid granular continuous phase, the air used for pumping the abrasive particles into the jet device was treated as a continuous phase and the water as a principle continuous phase. The governing equation were discretized using the finite volume approach, the solution was obtained using Euleurian model. The results clearly shows the effect of the taper inlet angles on the velocity of water, abrasive, air at the exit of the focus tube, and were compared with the experimental data.

Keywords: CFD, Euleurian, abrasive, velocity, turbulent model, taper inlet angle, multi-phase.

Résume:

Une méthode de calcul de la dynamique des fluides (CFD) a été développée pour découvrir la vitesse de l'air et de l'eau à la sortie du tube de focalisation, l'étude a été réalisée en utilisant une approche multi-phase, la particule abrasive a été traitée comme un solide Phase continue granulaire, l'air utilisé pour pomper les particules abrasives dans le dispositif à jet a été traité comme une phase continue et l'eau comme phase continue principale. L'équation de régulation a été discrétisée en utilisant l'approche du volume fini, la solution a été obtenue en utilisant le modèle Euleurian. La simulation a été effectuée en utilisant différents angles d'entrée coniques, les résultats montrent clairement l'effet des angles d'entrée coniques sur la vitesse à la sortie du tube de focalisation et ont été compares aux données expérimentales.

Mot clés: CFD, particules abrasive, Euleurian, turbulent, multi-phase, vitesse, angle d'entrée conique

التلخيص:

قد تم تطوير طريقة ديناميكية السوائل الحسابية (د.س.ح) لمعرفة الجسيمات والهواء وتوزيع المياه عند خروج أنبوب التركيز، وقد أجريت الدراسة باستخدام نهج متعدد المراحل، وتم التعامل مع الجسيمات الصلبة كمرحلة مستمرة، تم معاملة الهواء المستخدم لضخ الجسيمات الصلبة في الجهاز كمرحلة مستمرة والماء كمرحلة ابتدائية مستمرة. الحصول على الحل باستخدام نموذج يوليوريان. أجريت المحاكاة باستخدام زوايا مدخل مختلفة، والنتائج تظهر بوضوح تأثير زوايا مدخل على سرعة الماء، الجسيمات الصلبة، الهواء عند خروج أنبوب التركيز، وتمت مقارنتها مع البيانات التجريبية الموجودة في المرجع.

الكلمات المفتاحية: ديناميكية السوائل الحسابية،الجسيمات الصلبة،يوليوريان،كاي-ابلسيلون، السرعة، زوايا المدخل، متعدد المراحل.

CONTENTS

CONTENTS

Chapter II: State of art of AWJ machining

Chapter III: Computational modeling and method

Chapter IV: Simulation and interpretation of result

LIST OF SYMBOLS

Symbol	Designation	Unit
P_0	Atmospheric pressure	$[Pa]$
ρ	Density	$[Kg/m^3]$
V	Velocity of water jet	$[m/s]$
c	Velocity of sound	$[m/s]$
P_{abr}	Specific erosion capability of injection as well as suspension	$[-]$
a	Power exponent	$[-]$
Hp	Abrasive-material hardness	$[m]$
S	Abrasive-particle-shape	$[m^2]$
ρ_p	Abrasive-particle-density	$[Kg/m^3]$
d_p	Abrasive-particle-diameter	$[\mu m]$
m_A	Abrasive mass flow rate	$[Kg/min]$
α	Volume fraction	$[-]$
S_{mass}	Mass source term	$[m^2]$
Sp	Momentum source	$[N/m]$
F	Force preferred to fluid	$[N]$
ρ_K	Density	$[Kg/m^3]$
K	Gas, liquid, solid	$[-]$
μ_{eff}	Effective viscosity	$[N.s/m^2]$
g	Acceleration due to gravity	$[m/s^2]$
h	Height of the observed points above the reference plane	$[m]$
Ψ	Orifice parameter known as the coefficient of velocity	$[-]$
q_w	Volume flow rate of water	$[Lit/min]$

μ_t	Turbulent viscosity	$[m^2/s]$
Np	Number of phase	$[-]$
μ_α	Molecular viscosity	$[N.s/m^3]$
$c_{\alpha\beta}$	Inter phase heat transfer	$[J/Kg.K]$
K	Kinetic energy	$[J]$
ε	Dissipation rate	$[J/K_g.s]$
Lc	Length of mixing chamber	$[m]$
df	Focus tube diameter	$[m]$
θ	Inlet taper angle	$[degree]$
V_{w0}	Velocity of water at $x=0$	$[m/s]$
H_α	Static enthalpy	$[Kj/Kg]$

LIST OF FIGURES

LIST OF TABLES

INTRODUCTION

General introduction

In the early 1980's, abrasive water jet cutting system was established for its great advantages over alternative conventional cutting process. The abrasive water jet machining has accelerated and met the immense expansion of the many new applications; it has found its place in cutting metal composite material and rock cutting. In order to extend its application in manufacturing the influence of different parameters has to be sufficiently studied so that optimized parameters can be achieved.

The abrasive water jet work is to remove the target material mainly by impacts of abrasive material particles, it has a few advantages such as high machining flexibility, small forces high flexibility and no thermal distortion, and high cutting speed these are few of the advantages offered by this process for different application. Abrasive water jet machining process generally comprises of water pumping system, abrasive feed system, abrasive water jet nozzle and catcher. Pumping system delivers high velocity water by increasing pressure of a specific mass flow rate of water. It requires a high power motor connected to the intensifier with high intensification ratio.

Beside from abrasive carrier, water also acts as a cooling agent, and is used to flush away the eroded particle and to prevent the abrasive from wide spreading after exit from the nozzle (in some cases polymers are also added). Abrasives are fed to high velocity water by a precisely controlled orifice. As dry abrasives are difficult to feed a long distance, present researchers use abrasive-water mixed slurry to feed a long distance with higher power. Momentum transfer from water jet to abrasive and mixing operation takes place in nozzle.

The cutting of abrasive water jet depends on the mixing chamber length, taper inlet angle, focus tube diameter, focus tube length, orifice diameter and also abrasive inlet angle.

The object of this work was to know the effect that happens to the velocity if we changed the inlet taper angle; we took the taper inlet angle as our problem and the object of this work is to study the effect of the inlet taper angle on the velocity.

This master's thesis contains four chapters:

The first presents a literature review of pure water jet technology and abrasive water jet. It describes the process, its applications, principle, and industrial interest, as well as its characteristics and applications.

The second chapter is about a stat of art and the modeling in the point of view of researchers that studied the AWJM process on different materials and concluded different remarks on abrasive work piece interaction.

The third chapter deals with about modeling and state of some current work numerical simulation of water jet machining. It leads to the choice of the model adopted in the rest of the work of this thesis.

In the last chapter, the first steps leading to the simulation of an abrasive water jet cutting case are detailed: the models used to perform the multiphase flow simulation are presented, the simulations to arrive at the jet. The simulated case with the experiments will allow a comparative study in order to validate our simulation. At the end of this thesis, a general conclusion draws up an overall assessment of this work and the perspectives are presented.

CHAPTER I

Literature review

I.1. Introduction:

Water has long been known for its natural erosive effect, this natural erosion is found in the seas, rivers and caves where the rocks are carved by this caustic power native to our first source of life, in the last decade within the period of the last twenty years **[1]** or forty years ago **[2]**, there have been significant advances in the technology of abrasive water jet. A reduction in scale of this technology with smaller nozzle, higher water pressure and very fine abrasive make it become a new technology for micro fabrication **[3]**.

Abrasive water jet (AWJ) technology is a state-of-the art cutting tool used to machine a wide range of metals and non-metals, particularly " difficult to cut " materials such as ceramics and marbles, and layered composites, AWJ machining includes AWJ slotting, turning, drilling and milling**[4]**.

Nowadays, the term water jet jetting is usually appropriate for jet formed by water without any ingredients, on the contrary, the term abrasive water jet is used for water jets containing particles of solid matter added into them to increase of their efficiency **[1]**.

I.2. Abrasive water jet machining technology:

The technique of cutting materials using high pressure water jets was first time presented in 1968 by Dr Norman Franz **[20]** researcher at university of Michigan USA. In the early of 1970's, water cutting machines started to operate for cutting wood and plastics **[21]**.

It was soon discovered that the cutting process can be made more effective by introducing abrasives such as garnet into the water stream, the technology evolved abrasive water jet that use a high velocity coherent stream of water and abrasive that can be used to cut almost all materials **[7]**, however, this technology was not widely accepted by industry till the ultrahigh pressure pumps become commercially available in the mid of 1980's **[21]**.

In 1982, abrasive water jet was formed by entraining abrasive particles into a high speed water stream in a tubular abrasive nozzle, it was referred to (AIJ) abrasive injection jet, and in 1986 Fairhurt et al **[2]** reported a different method that was called abrasive suspension system (ASJ).

Today as one of the most recently developed non-traditional cutting process AWJ machining technology has been found to have extensive applications in manufacturing

industries for machining a wide range of metal and non-metal by using a fine jet of ultrahigh pressure water abrasive slurry.

I.2.1. Principle of AWJ machining:

Abrasive water jet machining is an emerging technology which enables the machining of practically all materials, due to advantage of AWJ machining such as no heat effect maneuverability, less machining force, this technique has been used in many industrial application**[5]**. A jet of water is generated by a high pressure pump, the compressed water acquires through a small diameter sapphire nozzle**[6]**, delivers high velocity water by increasing pressure of a specific mass flow rate of water **[5]**. Which can reach up to 1000 m/s, the value of this velocity is calculated using Bernoulli equation:

$$v = \sqrt{\frac{2(P_{water} - P_0)}{\rho_{water}}} \quad \text{(I.1)}$$

Where P water in the hydraulic pressure, P_0 is the atmospheric pressure, ρ water is the incompressible water mass **[22]**.

I.2.2. Description of AWJ process:

An abrasive water jet consists of a regular water jet with an abrasive added into the fluid (or mixing) nozzle, abrasive are particles of special materials like aluminum oxide, silicon carbide, sodium bicarbonate, dolomite or glass- beads with varying grain sizes, high pressure abrasive water jet cutting is essentially an erosion process which involves two distinct mechanisms depending upon whether the eroded material is brittle or ductile in nature **[23]**.

In these process the water acceleration at a 40.000 to 55.000 psi through a sapphire, ruby or diamond orifice. The stream passes through a mixing region where the vacuum, induced by the stream, sucks in abrasive momentum of the water stream acceleration and entrains abrasive asset passes through the nozzle (figure I.1). having received a lot of kinetic energy and velocity by water jet the stream exits the nozzle (carrying 0.5 to 1.5 pounds per minute of abrasive) as a three phase mixture of air, water and abrasive particles with a cutting diameter of 0.02 to 0.06, the high velocity abrasive particles impact on the kerf face and do the actual cutting, kerf material is removed as microchips, with no negligible effects on the material. To increase the flow of water we must increase the pressure and to do that we use two techniques that are:

1. The direct acting pump or triplex pump (three cylinders) which is actuated by a motor/belt assembly via a crankshaft, now days this technology is no used.

2. The intensifier or pressure-reducing system in the intensifier pump a hydraulic type primary circuit produces a flow of pressurized oil which is used to alternately actuate two opposing pistons these low pressure piston each push a high pressure piston which alternately compresses the water by means of a conventional system of intake / exhaust valves in the ration of their respective surface, which increase the flow of water, the movement of the piston is controlled by a control system **[19]**.

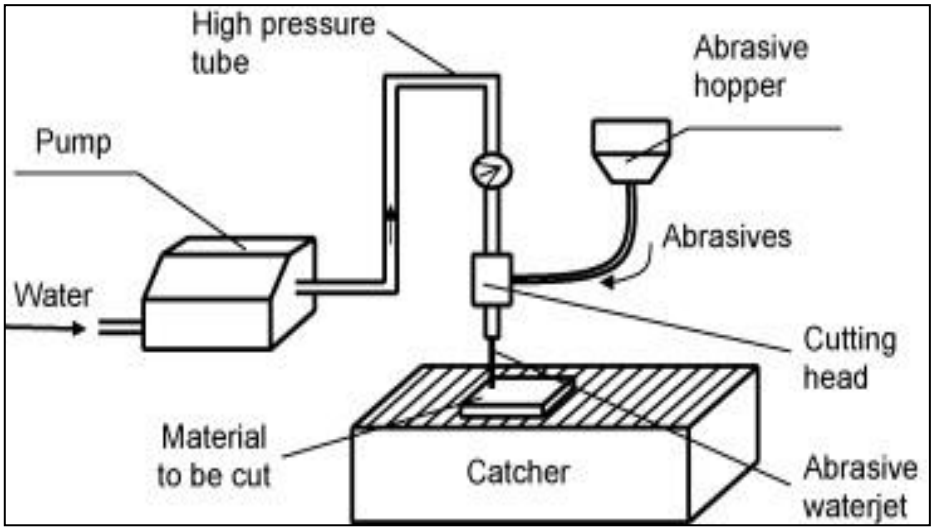

Figure I.1: *Schematic of an abrasive water jet cutting system.*

I.2.3. Characteristic of AWJ:

In the industries there are two types of machining that have almost the same process, we have water jet machining (WJM) and abrasive water jet (AWJ) they are two non-traditional or non-conventional machining processes They belong to mechanical group, the mechanical energy of water and abrasive phases are used to achieve material removal or machining, depending on the jetting and ambient pressure in ordinary pressure levels of water jet process, cavitations occurs in the region of high shear at the boundary between the jet and the surrounding water. Depending on the fluid medium jets are categorized as either pure water jet or abrasive water jet.

I.2.3.1. Pure water jet:

Consists of a stream of water without an abrasive material passed through a nozzle this type does not contain an abrasive agent, it is primarily used for surface cleaning and cutting of

softer materials **[2]**. The water jet passes through the nozzle at a high pressure about (100 to 400 MPa). The structure of water jet from velocity and pressure distribution point of view is presented in figure I.2.**[20]**

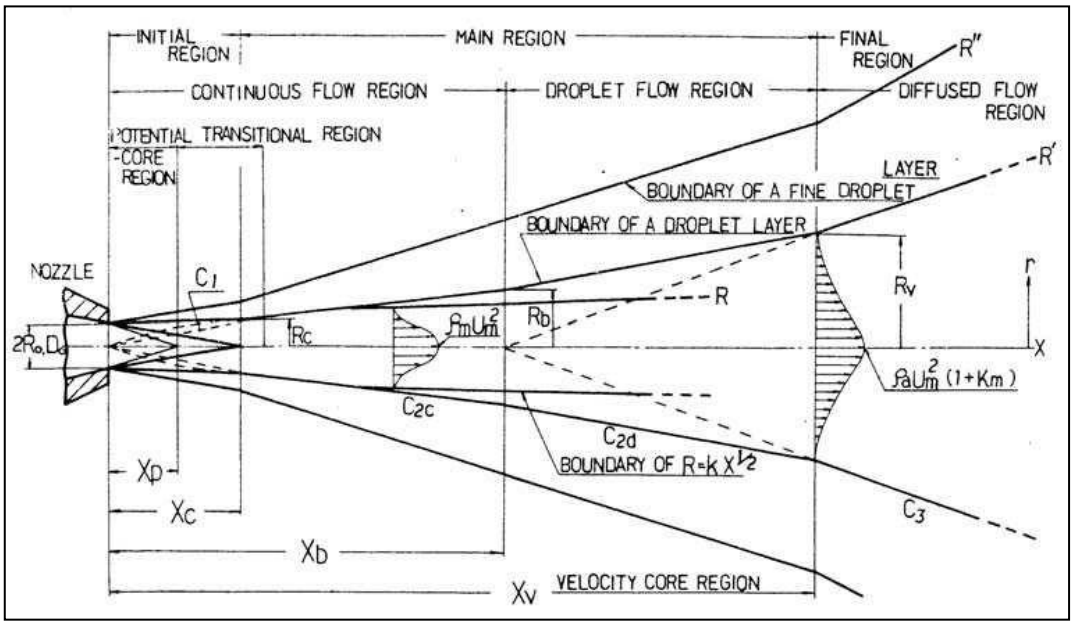

Figure I.2: *Structure of a high pressure water jet.* ***[2]***

The zone from above figure has the following characteristics:

1. Inside the initial zone, length X_b, the radial distribution of velocity (C_1) is constant and the same as those of exit from the nozzle, the length of the zone depend on the pressure and the diameter of the nozzle (d_0);

2. Inside the principal zone, length X_V, dynamic parameters of the jet varies on radial and axial direction, hence the velocity decreases up to value $C < C_1$ and the density of the core of the jet decreases;

3. Disintegration zone starts from the point where we have not a core of jet anymore.

There are two types of pressure that are formed from the contact of the water with the target material during the process. A stagnation pressure Ps is created at the impact point from a constantly flowing jet. A water hammer pressure P_W, is created instantly at the impact point if water droplets are formed in the jet, these pressures are responsible for the work that water jet does to the material if the pressure create local stress high enough to yield the material in the impact location, material removal will occur equation (I.2) and (I.3) below can be used to calculate these two pressures **[6]**.

$$P_S = \frac{\rho V_2}{2} \quad (I.2)$$

$$P_W = \rho C V \quad (I.3)$$

With:

ρ = Density of Water,

c = Velocity of Sound in Water,

V = Velocity of Water Jet.

Since the velocity of sound in water at normal temperature and atmospheric pressure is approximately 1,500 m/s, the water hammer pressure pw is much larger than the stagnation pressure P_s under ordinary impact conditions.

I.2.3.2. Abrasive water jet:

Abrasive water jet is a polyphasic fluid where the constituents do not react chemically each other, the phases of this fluid are:

1. A liquid phase represented by the water (with the largest mass participation);
2. A solid phase represented by abrasive particles;
3. A gaseous phase represented by the air introduced in fluid due to method of introduction of abrasive particles in water jet (injection).

In figure I.3 we show the mechanism of abrasive particles in water jet.

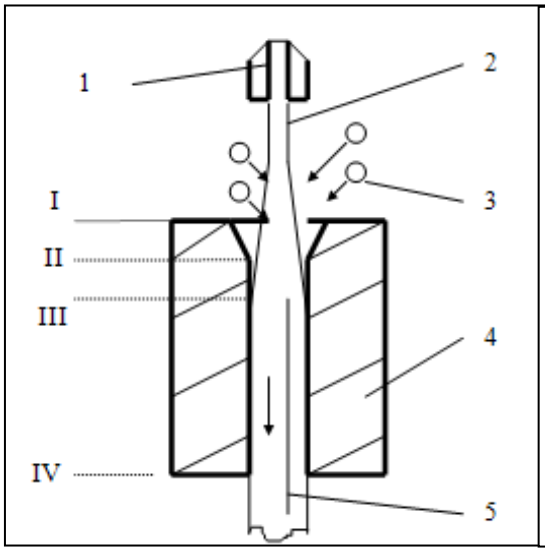

1 – Water jet nozzle;

2 – Formed water jet;

3 – Abrasive particle;

4 – water – abrasive particles focus;

5 – Formed abrasive water jet.

Figure I.3: *Abrasive water jet forming mechanism.*

The high pressure water jet 2 passes thru a zone called mixing chamber between nozzle 1 exit and entrance in focus 4. In this area the pressure is negative due to very high velocity of water jet.

Abrasive particles 3 are sucked in water stream due to this negative pressure, in area ranging between points I and II. In area between points II and III the abrasive particles are forced to move in the direction of the water stream, but the velocity of them is low. If the abrasive jet should exit from focus in point III, the velocity is too low and the efficiency should be low also.

Between points III and IV the abrasive particles velocity is increased but this will never reaches the velocity of water jet. If the length of this zone is too big, the velocity of particles will be decreased due to friction with focus walls. Because there are so many parameters, it is difficult to theoretically determine the length of focus 4. Hence the length of focus is experimentally determined by the focus Manufacturers in order to increase as much as possible the velocity of abrasive particles **[20]**.

I.3.Generation of AWJ:

I.3.1. Structure of high speed fluid jet:

I.3.1.1. Classification of high speed fluid jets:

The term "high speed water jet "includes several modifications of jets shown in figure I.4. it is technically difficult to define a critical pump pressure that separates a low pressures jet and a high pressure jet , Louis suggested that jets generated by plunger pumps should be defined as "low pressure jet", whereas jet generated by hydraulically driven intensifiers (**figure I.5**) are called "high pressure jet" these definitions create several problems because recently developed commercial plunger pumps are able to generate water pressure up to 270 MPa which is in the range of hydraulic pressure intensifier **[24]**.

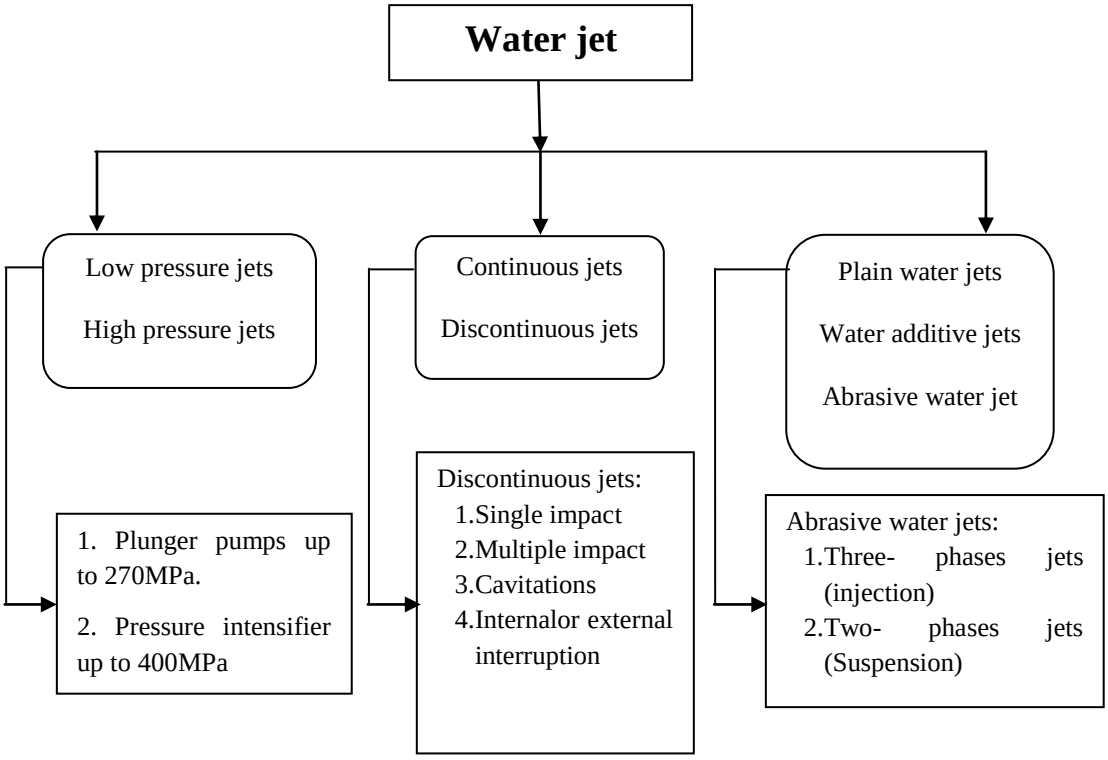

Figure I.4: *subdivision of water jets.*

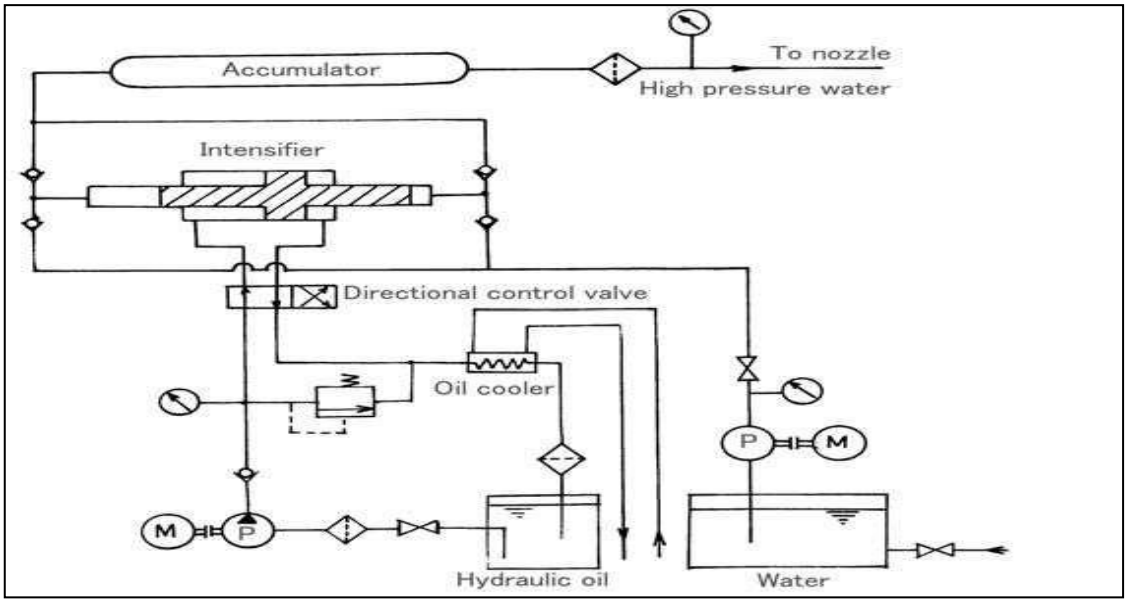

Figure I.5: *Circuit of the intensifier pump* ***[2]***

I.3.1.2. Velocity of High-Speed Water Jets:

1. **Air**:

Air is one of the three components of the abrasive water jet. The amount of air is the dominant amount of the abrasive water jet. According to Mr.Zaki **[13]** air represents 90% of

the volume of the three-phase jet. Nevertheless, air does not produce practically no mechanical action and thus does not contribute to the removal of material on the part.

2. **Water:**

The water used in this technology is water from the profiteered network (particle size m) before entering the pump.µGreater than 10 it is then filtered twice at the input of the pump by two filters, one of 1µm and the other of 0.5µm. This filtering system Eliminates macros and micro-molecules that can clog pumping and deteriorate the pump **[14]**.

3. **Abrasive:**

Abrasives are natural or synthetic materials capable of exerting an action Mechanical means for removing material in the form of tiny chips. the characteristics affecting abrasives on the removal of Materials are mainly: the shape, the nature, the hardness and the density of the abrasive.

4. **Pressure:**

The water acquires its potential energy by a pump generating a pressure. This one Up to 4000 bars for piston pumps and 6000 bars for axial piston pumps generally consist of three Connecting rods and cranks. The boosters are pressure multipliers which ensure Transmission of pressure from a hydraulic (oil) circuit to a water circuit. A Piston actuated by a hydraulic fluid is connected to another smaller piston Diameter which generates the pressure of the water (Figure I.6). Thus, the value of the pressure of the outlet water is that of the oil multiplied by the ratio of the surfaces between the sections of the two pistons **[10]**.

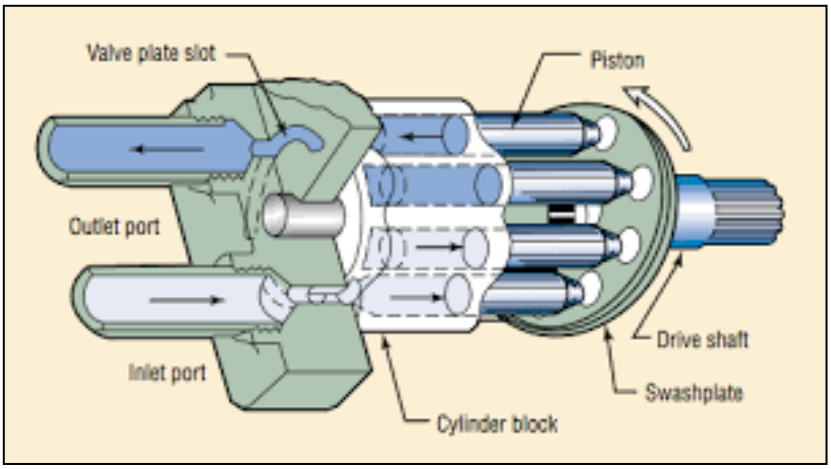

Figure I.6: *Operation of an axial piston pump.*

5. **The nozzle:**

The nozzle makes it possible to transform the pressure exerted on the water particles in speed. The nozzles consist of a diamond, ruby or sapphire orifice and the conical shape of the Stainless steel hole allows for centering on the cutting head.

6. **Feed rate:**

The feed speed (mm / min) represents the relative speed between the cutting head and the machined part. It's one of the most influential parameters in technology AWJ. Many studies use the influence of forward speed on the depth of chopped off. Hascalik**[16]** studies the influence of this parameter on the depth of cut of a 5 mm thick Ti6Al4V plate. By selecting a pressure of 1500 bar, an impact angle of 90 °, a firing distance of 3 mm and an abrasive flow of 0.005 kg/s.

7. **Shooting distance:**

Generally, the firing distance used in cutting is of the order of 3 mm to ensure a Homogeneous section with the coherent jet zone. The abrasive flow rate is defined by the mass of the abrasive particles impacting the work piece by Unit of time. This parameter is controlled by a pellet through which Pass the abrasive particles and then traverse the abrasive feed pipe and finally discharge into the mixing chamber. The diameter of the abrasive pellet defines the Mass flow of abrasive.

I.3.1.3. High Pressure Water Jet System:

An ultra-high pressure system manufactured by Dardi International Corporation of China served as the source of high pressure in the experiment. With a single intensifier, a maximum jet pressure of 380 MPa could be reached. The primary operating parameters of the system are listed in Table 1. The nozzle was fixed at a supporting frame, whose traverse and vertical displacement were accurately manipulated through a digital control panel **[25]**.

Parameter	Description
Pressurization ratio	20:1
Power	30 kW (50 Hz)
Maximum	380 MPa
discharge pressure	3.7 L/min

Table I.1: *Primary operating parameters of the ultra-high pressure system.*

I.3.2. AWJ system:

Abrasive water jet is classified as either abrasive suspension jet (AIJ's) or abrasive suspension jet (ASJ's) based on the generation mechanism and the phase composition:

I.3.2.1. Injection jet:

The injection water jet cutting process works by creating a high pressure stream of plain water via a pump with pressures ranging from 100MPa to 400MPa, a stream of fine grained abrasive material is accelerated toward the cutting head (low pressured). The stream of water and abrasive material enter the cutting head separately, the mixing of the water and abrasive accurse in a mixing chamber. The abrasive material in "injected" into the high pressure stream of water, the low pressure in the chamber allows for air to mix with the water and abrasive material. This create an abrasive slurry resulting in roughly **90% air**, **6% water** , **4% abrasive** that then enters a focusing nozzle, this mixture leaves the nozzle at velocities in the order of magnitude of 100 meters per second**[6]**.

I.3.2.2. Suspension jet:

It differs from the injection water jet , in this method the nozzle create a result of **90%water** and **10% abrasive**, there are three different type of suspension AWJ formed by direct , indirect and Bypass pumping shown in figure I.7**[26].**

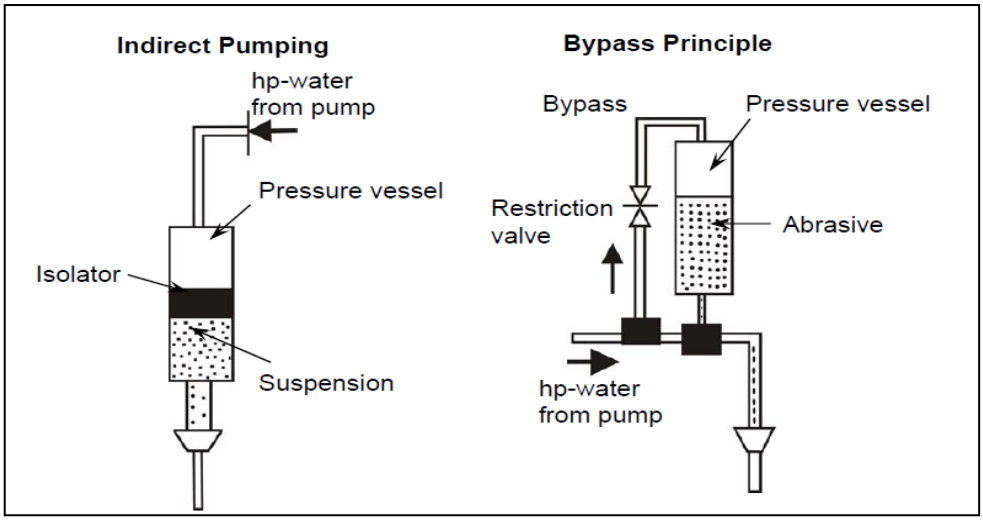

Figure I.7: *Schematic of AWJ suspension type.*

The abrasive material is suspended in a storage vessel and is held under pressure which in turn is allowed to discharge from a nozzle to form abrasive water jet with a lower pressure than that of the injection water jet, In fact **[27]**:

1. An abrasive suspension jet consists of two components only water and abrasive;
2. Radial dispersion of solid particles is smaller and it can be further reduced by adding suitable chemicals;
3. The abrasive load is quite large (up to 10 kg/min) allowing deeper cuts to be achieved with higher cutting rate compared the injection method;
4. The pump is operated at relatively low pressure (up to 70MPa);
5. The nozzle can be oriented in every direction under appropriate safety requirement.

I.4. Technology with AWJ cutting:

Water jet cutting (WJC) involves the removal of material by directing a thin, high velocity jet of water to the work piece, pure water jet can efficiently cut variety of materials such as corrugated box board, paper, plastics, leathers, circuit boards…etc.

I.4.1. AWJ cutting:

Pure water jet is not capable of cutting harder materials, mixing of abrasive particles with the high velocity water jet is an excellent way to increase the cutting capabilities of water jets this is called abrasive water jet cutting , it can cut harder materials which include super

alloys, composites titanium ceramic, carbon and stainless steel, glass and concrete. WJC has become a versatile tool for many applications such as rocks cutting, mining, drilling and deep water cutting for off shore operation **[29]**.

I.4.1.1. Erosion cutting:

Erosion cutting is the result of successive impacts of abrasive particles, which move at high speed on the material of the work piece all the pieces especially metallic ones are cut according to the same mechanisms and the parameters of cut **[30]**. Generally it divided into two groups, the input and output parameters **[21]**:

1. **Input parameters:**

Hydraulic parameters	**Cutting parameters**
*Water jet pressure *Water diameter	*Travers speed *Standoff distance *Angle of attack
Target material	
*Fracture strength *Hardness *ductility	**Abrasive parameters**
	*Abrasive particle size *Abrasive material *Abrasive flow rate *Abrasive condition (dry or slurry
Mixing parameters	
*Mixing diameter *Mixing tube length	

2. **Output parameters:**

Kerf characteristics	**Geometrical and dimensional accuracy**
*Surface waviness *Kerf width and taper burr formation surface finish depth of cut	**Material removal rate**

I.4.1.2. AWJ cutting mechanism:

Abrasive water jet cutting make use of high velocity water entrained with abrasive particles to cut different materials ranging from soft, ductile to hard and brittle materials it is a non-contact, inertia-less process that offers several advantages like narrow kerf width,

negligible heat effect zone, though it is capable of cutting different materials of different thickness the extent of penetration of the jet into the material depends on various process parameters and material properties.

Generally, in abrasive water jet cutting, catcher tanks serve mainly two purposes. First, they hold and support the work piece and second, they capture the dispensed abrasive and water from the cutting nozzle including any effluents **[11]**.

In another hand, each of the cutting head efficiency (Table I.2) is evaluated in a pristine condition. By analyzing the "throw distance" of the abrasive particles at three pressures and at three abrasive feed rates **[12]**.

Elements of the Cutting head	**Function**
Collimation tube	Produce a regular water inlet to the nozzle
Nozzle	Transforming the potential energy (pressure) of water into energy (Speed) of the jet. Its shape determines the diameter of the jet and its coherence**[10]**
Mixing chamber	Allow a mixture of water and particles of aspirated abrasives in the jet.
Head Body	Connect the components of the cutting head
Lock Nut	Tighten the focusing tube to the mixing chamber
Cannonball(Focusing)	Contain particles in the jet during acceleration and Focus the jet by forcing it to follow its axis.

Table I.2: *Cutting head components and their functions.*

1. Cut geometry:

Abrasive water jet cuts have straight width with a slight amount of taper kerf width is controlled by orifice/nozzle combination cuts in thicker materials geometry require larger combination with more abrasive usage. The kerf width can be as small as 0.020" for thin materials and up to 0.055" in thick materials. The minimum inside corner radius is controlled by the nozzle diameter and therefore is 0.010" to 0.030". Inside corners may have digs on the bottom of the cut in thick materials.

This is due to the exit of the stream lagging behind the entrance side of the stream and can occur as the jet exits from corners. Reducing the feed rate or adding a radius of at least 0.5" can eliminate this in thick materials. Abrasive jet can slice or drill holes smaller than 0.060" diameter.

2. Cut quality:

Cut quality describes the kerf edge and taper. The feed rate controls the amount of jet lag. Cutting speed and edge quality are directly related at the high feed rates the jet has increased curvature as it passes through the cut. Reduced cutting speed can result in a good edge finish of 125 micro inches, having a ground appearance and minimal taper high feed rates for separation cuts give striations through the full cut **[17]**.

I.4.2. Classification and characterization of abrasive materials:

I.4.2.1. Type of abrasive materials:

A large of different types of abrasive materials is used in the abrasive water jet technique. A survey in 1995 shows that most of the abrasive water jet shops use garnet (90%) followed by olivine (15%), slag (15%), aluminum-oxide (11%), and silica-sand (11%). Martinec distinguishes between two major groups of abrasive materials-oxides and silicates (tableI.3).

Oxide	**Silicate**	
	Garnet	**Other silicate**
Magnitude	Almandine	Zircon
Ilmenide	Spessartine	Topaz
corundum	Porype	Olivine
Retile	Grossularite	Staurelite
Quartz	Andradite	Olivine

Table I.3: *Type of abrasive particles.*

Agus et al introduce a parameter to evaluate abrasive material **[24]**:

$$P_{abr} = H_P^{a1} \times S^{a2} \times \rho_P^{a3} \times d_P^{a4} \times m_A^{a5} \quad \text{(I.4)}$$

That includes the following parameters:

1. Abrasive-material hardness;
2. Abrasive-particle shape;
3. Abrasive-material density;
4. Abrasive-particles diameter;
5. Abrasive-mass flow rate.

P_{abr} **:** Specific erosion capability of injection AWJ as well as of suspension AWJ.

In the table I.4 have the different value that can the power exponent take for the different parameters

	Power exponent				
Target material	**a1**	**a2**	**a3**	**a4**	**a5**
Granite	1.4	0.2	-0.4	0.1	-0.5
Porphyry	1.5	-0.1	-0.2	0.1	-0.5
Basalt	1.2	0.7	-0.2	0.1	-0.5
Marble	0.7	2.0	-0.2	0.1	-0.5

Table I.4: *Abrasive-material characterization exponents* ***[25].***

I.4.2.2. Distribution of particles in the jet:

Assumptions about the distribution of abrasive particles in the water jet are contradictory (this is probably due to different experimental conditions such as the shape of the mixing chamber and the greater or lesser concentration of the particles).

Indeed, hashish observed that the particles are concentrated in the central part of the jet. Moreover, abdaka states that the particles are more numerous in the periphery, at the centre of the jet, and particles fall freely from the focusing tube, on the other hand Gaskin and Chen observed that the turbulent diffusion of the jet distribution of the abrasive particles changes randomly along the mixing process.

In AWJ cutting, abrasive particles perform the actual cutting action while the high velocity water jet accelerates them to the required velocity to enable the cutting. Because of the inefficiency of conventional abrasive entrainment 70 to 80% of the abrasive particles are fragmented during the mixing and ejection process.

I.5. Application:

Abrasive water jet has the ability to cut almost all materials and thicknesses. Most uses are for cutting of specialty materials such as stainless steel and aluminum. Its flexibility makes it useful for all applications, but of course some uses are better than others. The following is a list of applications where water jet is the best approach:

- Shape cutting of $1/4''$ and thicker aluminum
- Net size cutting of $1/2''$ and thicker stainless steel
- Blank cutting of parts for final machining
- Short run lots of sheet metal parts
- Screen Cutting
- Converting plate stock to bars
- Precision cuts in $1/2''$ and thicker mild steel
- Hardened materials
- Intricate shapes in delicate materials
- Custom shims in stainless steel and exotic materials
- Tube cutting

Note that conventional applications such as sheet metal and low accuracy mild steel cutting are not on this list. Abrasive water jet can do this with quality results but, generally is too expensive compared to plasma, laser or punching **[17]**. The present process has the advantage of using a clean fluid which allows its use in the agro-food and even medical field. Finally, it can be added that, despite the high operating pressure of the pump which propels the jet (up to 4000 bar), the pressurized tanks remain relatively unsafe due to the low compressibility of the water.

I.6. Conclusion:

The AWJ has allowed the cutting of hard materials with very high mechanical properties such as stainless steel, titanium and inconel. In addition to its main application, this technology can be used for a multitude of functions and applications (drilling, stripping, polishing ...). To arrive at these applications, a great number of studies, observations, experiments and simulations have been carried out since the 1950s and this continues in evidence all theses and articles published in this field.

CHAPTRE II

STATE OF ART OF

AWJ MACHINING

II.1. Introduction:

To be able to study and improve any process, we must make a theoretical representation of a system of elements and relations more or less complex, called modeling. Modeling of experimental observation and prediction of responses through that model are highly relevant for study the influence of parameters on any process.

Previous modeling work are broadly classified into six grouped **[5]**(**figureII.1**).but in actual case the abrasive water jet encompass the flow of three phases (water, air, solid) , most researchers have carried out experiments for the abrasive particles and water, since it's difficult to measure the velocity of air at the exit of the focus tube**[2]**. There have been significant contributions in this AWJM process, researchers generally try to develop a model for the responses of the process. Still no such model is found to exactly predict this process out puts. Assumptions considered by researchers' deviates them from real world applications. There for, further study is needed to explore the underlying mechanism of this process to predict the responses more accurately. Researchers investigated the AWJM process from different point of view and concluded a number of remarks regarding the different aspect of the process. Findings from different work are broadly classified in modeling, parametric study and optimization.

II.2. Process:

AWJM is an emerging technology with enables the machining of practically all materials due to advantages of AWJM such as no heat effect zone, and ability to cut harder materials, high degree of maneuverability. Less machining force this technique has been used in many industrial applications. Like other high energy beam cutting techniques, AWJ cutting may cause striation marks on cut surface finish. AWJM process generally comprises of water pumping system, abrasive feed system, AWJ nozzle and catcher **[37]**. Pumping system delivers high velocity water by increasing pressure of a specific mass flow rate of water.

It needs a high power motor connected to the intensifier with high intensification ratio. Abrasives are feed to high velocity water by a precisely controlled orifice. As a dry abrasive are difficult to feed to long distance, present researchers use abrasive–water mixed slurry to feed a long distance with high power. Generally, nozzles are the place where the mixing operation of water jet and the abrasives happened, and they are made from high wear resistant materials like sapphire.

There are 2 types of mixing operations, abrasives are feed through a conical zone to the water passing through the center, but it doesn't take high mixing ratio, another one is where water is supplied to centrally flown abrasives. After cutting, the work piece high velocity water filled open chamber kept just below the work piece **[5]**.

II.3. Modeling:

Modeling of experimental observations and prediction of responses though that model is highly relevant for studying the influence of parameters on any process. There are number of techniques to develop a model that will represent the process. Models will be effective in prediction in practical field of work if that model validate with high correlation coefficient to the numerical results found in experimental runs. In this study previous modeling works on AWJ process are broadly classified into 6 groups:

1- *Numerical modeling;*
2- *Differential equation based modeling;*
3- *Analytical modeling;*
4- *Statically modeling;*
5- *Models developed by dimensional analysis;*
6- *Neural network modeling.*

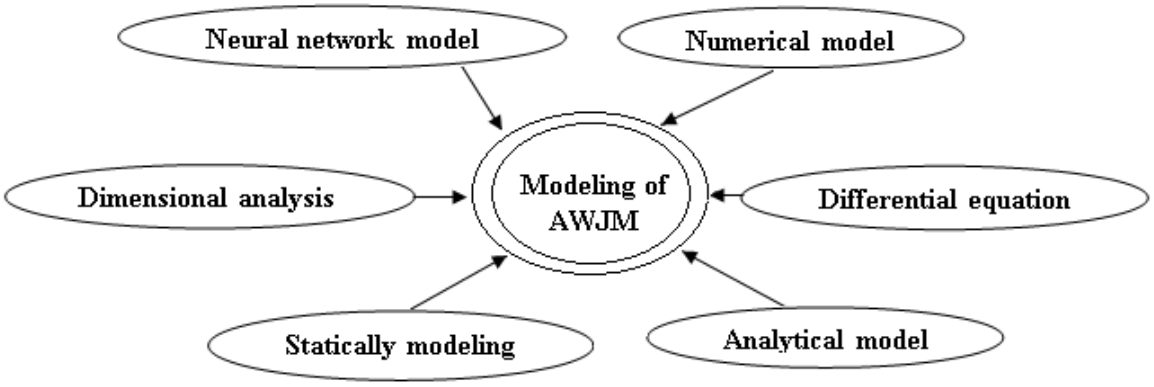

Figure II.1: *Modeling techniques applied for AWJM process.*

Modeling of material removal rate, surface roughness, depths of cut, kerf taper, are generally done using mostly in the input parameters. Water pressure, abrasive mass flow rate, traverse speed and standoff distance. Numerical models are developed based on finite element analysis or CFD simulations.

Differential equation based models are to be solved to predict different responses. Different mechanisms of cutting operation are considered for developing analytical models, whereas, statically modeling was done based on experimental results.

Some models are built by dimensional analysis and coefficients are calculated from experimental readings. Another modeling technique neural Network is also taken into account by some researchers.

II.3.1. Numerical modeling:

Surface displacements of specific work piece materials were discussed through moiré fringes and contour plots as well as by FEA models **[38]** assuming impact on target materials as a similar as static loading on work piece material though finite element modeling of the interaction between jet and work piece in AWJ. Hassan et al **[39]** concluded that pure water jet had no ability to deform metals even at 350 MPa except generating micro pits. Li et al presented ultrahigh velocity water jet and AWJ through CFD simulation.

They discussed rapid decay of axial velocity of particle and fluid phase in "initial region" and top that profile of jet cross-section witch highly influences the kerfs profile in work piece material **[5]**. Jankar et al **[40]** studied the effect of velocity and impact angle of single abrasive particle on material erosion by considering the crater sphericity through FEA analysis. It was found that the erosion process is more unpredictable in case of small abrasive particles with low velocity. Erosive behavior in ductile and brittle material was modeled through FEA by Wang et al **[41]** using the previously developed models erosion rates revealed by this model are found to be consistent to particle results.

Wang **[42]** almost accurately predicted the velocity distribution inside the jet by considering dynamic characteristics of jet using CFD simulation study. How techniques of FEM, element erosion and adaptive meshing was implemented to deal the large deformation problem and damage modeling of ductile material machined by AWJ , Takaffoli et al **[43]**; Investigated the behavior of maximum depth of foot print, and erosion rate of elasto-plastic materials by non spherical particles using FE modeling.

To emulate the real interaction of AWJ with work piece material, that model incorporate the effects of strain rate sensitivity. Adiabatic heating and friction behavior in erosion process, 3D erosion modeling of crater geometry generated by multiple particle impact on elasto-plastic

material varying different impact velocity and angle through FE modeling was studied by Kumar et al **[40]**.

II.3.2. Differential equation based modeling:

Vikram et al **[41]** developed a differential equation based model for predicting surface topography by simulating the equation of trajectory of the jet. They used theory of ballistics, Bitters theory of erosion and found that the jet trajectory is curvilinear. Highly random nature of striking the abrasive particles was discussed through power spectral density analysis. This random nature of cut surface was generated due to inter section of striation marks and steps formed by trajectories.

Model suggested by Deam et al concluded that though jet trajectories are always trying to make a constant radius of curvature for through cuts, but no-local effects of curvature variation of the cutting face is almost unavoidable even after precisely controlling the cutting parameters. Their model was based on the assumptions that wear or cutting at a point depends on both local and upstream condition, but that can be extended from steady state to transient conditions **[5]**.

A two-fluid model (particles were considered as pseudo fluid) developed by Wang et al showed that intense turbulent shear layer is formed in both radial and axial direction between slurry jet layer and water at outer fluid-field due to momentum transportation and energy dissipation. From their model a clear idea is found regarding the nature of distribution of radial and axial velocities of this tow phases at different standoff distances. Geometry of jet foot prints is very important especially for control-depth cutting milling operation **[5]**.

Axinte et al. **[41]** and Kong et al **[43]** Predicted these foot prints at different working conditions. Both of them related the foot point geometry to the specific etching rate for different jet-work piece combination though Axinteet al model was restricted to 90° jet Impact angle, but the model by Kong et al described the path of restrained jet in any type of work piece with different impact angles. This model may also be applied for other energy beam (dwell time dependent) material removal processes.

II.3.3. Analytical modeling:

Hashish **[26]** elaborately studied the effect of variation of four most influencing control parameters (water pressure, abrasive mass flow rate, traverse speed and stand of distance) on depth of cut, surface roughness and finally suggested a simple model of depth of cut with those control parameters. In that study wear of mixing tube, water jet solid mixing, and abrasive transport were not considered. Chen et al developed two models of depth of cut: One for total depth of cut; another of taper zone in 87% alumina ceramic.

They divided total depth of out cut into three zones and claimed characteristics of these 3 zones are highly dependent on water pressure and traverse speed. Soires et al continued this study for the same material and developed models for depth of cut.

Both of their models fit good to experimental results. The depth of smooth zone can be increased up to 30% by forward oscillation in the plane of cut **[5]**. El-domiaty et al developed depth of cut models for brittle materials (considering fracture toughness and hardness of ceramic material) assuming two different conditions, but both of them predicted almost in similar fashion with high correlation coefficient (0.95) and less error (about 10%) to practical results in case of first model, they assumed that, plastic deformation contributed to the process of crack propagation and surface shipping, and erosion rat proportional to material removed by each impact. In the second model they assumed that lateral crack size is proportional to the maximum particle penetration.

Abdel-Rahman et al continued that study and their model validated the practical results with average error 4.5% for alumina ceramic **[5]**. Their model showed same trends as well know Hashish's model. Wang Conduced experiment for modeling of depth of jet penetration on polymer matrix composite varies the jet impact angle. It was finally concluded that in upper zone ploughing and shearing are dominant whereas main cutting accrued at lower zone with some fibers are pulled out leaving hairline burrs on cut surface.

II.3.4. Statically modeling:

In rectangular pocket milling, variation of depth is an obvious problem in AWJM. Paul et al empirically developed model for this variation in C-37 steel. They reported that the effect of variation of standoff distance is very low and by their model variation can be controlled within 0.04 mm with an acceptable surface finish. **[5]**

Wang et al found that during cutting of steel, micromachining and plastic deformation play dominate role in developing kerf geometry and surface roughness of cut wall. Surface roughness can be improved up to 30% by oscillating the nozzle heat with high oscillation angle and low frequency in case of cutting mild steel **[5]**.

Implementing nozzle head oscillation Lemma et al proved that surface quality will be improved up to 20% in case glass fiber reinforced polymer composite materials. They also stated the negative effect of higher oscillation frequency and lower angle of oscillation.

Though surface quality is getting reduced at high frequency of oscillation but depth of cut will be improved significantly at higher frequency (around 5-10 Hz) and low angle of oscillation. Lemma et al **[45]** found that depth of cut is increased 30% for mild steel, and 20% for aluminum. In case of glass epoxy composite. Azmir et al experimentally proved that part from operation control parameters, form of fiber and thickness of laminate have significant effects on roughness value instead of fiber volume fraction.

Azmir et al, also suggested that increasing kinetic energy of get caused deter quality of cut on kelvar-phenolic composites. Higher traverse speed favors for surface quality at the cost of sacrificing depth of cut. He didn't found any role of abrasive mass flow rate on roughness value, but selvan et al proved negative effect of abrasive mass flow rate on surface roughness and positive effect on depth of cut. **[5]**

Analysis of kerf characteristics from a completely different angle was done by Ma et al they compare the kerf profile developed when fluid flow enters a pipe from large tank. In the first region (entry zone: around 2 mm for acrylic) I. e developing stage, velocity profile of the jet changes from a uniform profile to a fully developed flow in a groove and the shape of the next region depends on cutting speed as lower speed opens out the groove. Nozzle wear phenomenon was investigated by Nanduri et al. **[5]**.

II.3.5. Dimensional analysis:

As coefficients of the dimensional analysis based models are calculated from experimental investigation so applicability of the models has become limited to that experimental conditions specifically for that material.

Xu et al developed a dimensional analysis based model for alumina ceramic with nozzle oscillation and that model predicts depth of cut within 3.3% mean error.

They also reported that cutting with nozzle oscillation within specific frequency and oscillation angle zone depth of cut will be increasing up to 82% than normal cutting.

J.Wang **[4]** further modified that mode introducing tow another material properties namely material flow stress and dynamic hardness of alumina ceramic. As a result mean percentage error in predicting goes (about 1%). Later experiments conducted by Wang, for multi-pass cutting with nozzle oscillation, in alumina ceramic.

It was observed that depth of cut increases up to 50.8% than single-pass cut. Also knops hardness and fracture toughness of work piece material were introduced in the model and prediction error remains about 1% **[5]**.Apart from brittle Alumina ceramic, modeling of kerf characteristics and delaminating in inhomogeneous layered composites were also done. Shanmugam et al **[5]** developed a model for kerf taper in cutting of two types of composites : epoxy pre-impregnated graphite woven fabric and glass epoxy from energy conservation approach assuming velocity of particles are same as jet velocity and only the particles energy is contributed for material removal process. Average % error value within 4_6 indicates their models adequacy based on energy conservation approach maximum crack length generated in graphite epoxy composite was modeled by Shanmugam et al It was claimed that delaminating is initiated by shock wave impact and propagated as a result of slurry jet penetration into crack tops that promotes water-wedging and abrasive embedment. ANN optimum control parameters are set by simulated annealing with function value predicted considered. Finally it was concluded that integrated model is more accurate than pure ANN model for predicting surface roughness **[5]**.

II.3.6. Neural network modeling:

Neural networks models were used to predict depth of cut, surface roughness and material removal. Back propagation neural network (BPNN) with sigmoid transfer function was commonly employed in all cases. For modeling depth of cut **[5]** inputs of neural network were chosen by genetic algorithm. Two cases studies were done; first one was to choose the process parameters to achieve a desired depth of cut with a fixed nozzle diameter; in other case, nozzle diameter as a variable control parameter. In both the cases correlation coefficients were found too high to use this model in practical use. In that study it was also compared that the used neuro-genetic approach is better than fuzzy genetic approach.

In case of modeling material removal rate, Addition to BPNN (Back propagation neural network) radial basis function net work (RBFN) with Gaussian kernel function as transfer function was also considered. 3-4-4 BPNN structures with constant learning rate of 0.4, 500 epochs and 3-10-4 RBFN network with constant learning rate of 0.3 momentum term of 0.7, 300 epochs were finally selected for predicting MRR. **[5]**

A final conclusion was drawn that RBFN network model more accurately predicts than BPNN and regression model. Caydas et al used three types used three types of sigmoid functions for predicting surface roughness and compared that to regression model.

In other model of surface roughness simulated annealing was integrated to ANN optimum control parameters are set by simulated annealing with function value predicted through ANN model. Two types of integrations were considered. Finally it was concluded that integrated model is more accurate than pure ANN model for predicting surface roughness. **[5]**

II.4. Material application:

Abrasive water jet machining process is generally applied for slicing on difficult to cut, non conductive materials. Energy required for machining is varied from material to material. Harder material required huge energy than relatively soft materials. Amount of taper kerf width, depth of cut, surface roughness, material removal rate etc…. Such responses depend not only on energy supplied by slurry jet but also on both work piece and abrasive material properties. Mostly used abrasives different types of garnet (Almandine, olivine, Idaho.) with different grit sizes (#60, #80, #120 etc).Besides, corundum, sic, alumina, B_4C etc are also considered as for different abrasive work piece material combination. Abrasive material should be harder and wear resistant than target material. Besides, sharp particles are always preferred for erosive action. It was reported that for refractory ceramics corundum is more erosive than garnet. **[5]**Different researchers study the effect of control parameters on different types of work piece materials chosen by its availability and applicability. A relative use of materials is shown in **figure II.2**.

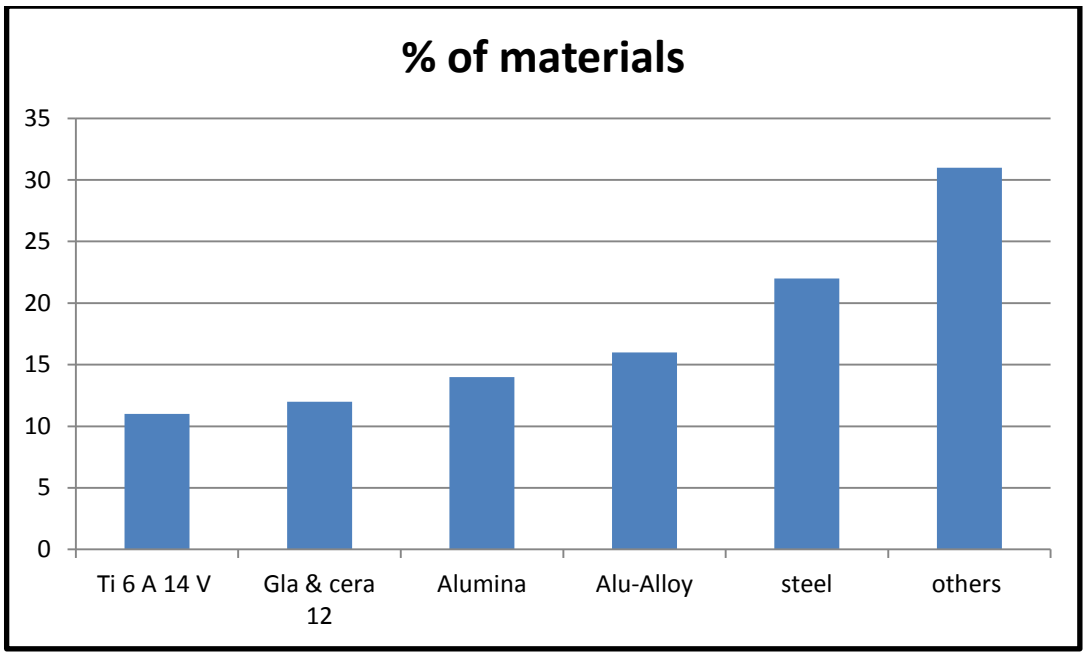

Figure II.2: *Work piece materials use in AWJM.*

Different grades of steel are extensively used for experimental work. Alumina alloy and 87% alumina are also considered for investigation. A part from these Ti6A14V, brittle glass and ceramic and various composites are taken for experimental study.

II.5. Parametric study:

Researchers considered a plenty of input and output parameters for experimentation. Almost all input& output parameters are lasted in **figII.3**. Among them water pressure, abrasive masse flow rate, traverse speed and standoff distance are the most influencing control variables. As AWJM is generally used for cutting purpose, depth of cut, surface finish, kerf taper are taken as responses.

From literature survey, it is found that increase in water pressure and abrasive mass flow rate generally cause higher depth of cut whereas, lower values of traverse speed, and standoff distance favors in increasing depth cut. Again, water pressure and abrasive mass flow rate inversely effect and traverse speed and standoff distance directly affect kerf taper ratio. Standoff distance has a strong positive influence on kerf width. As traverse speed increases, surface roughness and material removal rate both decreases.

Some researchers experimentally established that kerf taper will be significantly reduced by oscillating the nozzle with in a specific range of frequency and angle of oscillation. Shanmugan suggested that inclining the nozzle in a plane perpendicular to cutting direction,

one side taper can be almost eliminated. **[5]** For fiber reinforced composites, it was reported that form of fiber and laminate thickness are the most significant noise factors for the study of the surface roughness, whereas fiber volume fraction has no significant effect on roughness value. They reported that there exists a critical local exposure time witch depends on compressive strength and resistant to cut value of the target material. Above that critical value, erosion rate stable but below witch erosion rate rapidly increases.

Wang et al **[4]** studied the burr formation in through AWJ cutting of coasted sheet steel. They found that as the traverse speed and standoff distance decreases, burr height also decreases, whereas abrasive mass flow has no significant effect on burr height. A few researchers studied the change of depth of cut after multiple pass within the time of single pass. All of them reported that depth of cut is significantly increased with higher number of pass, actual cutting time and cost both can be reduced. Additionally, Wang et al concluded that multiple passes reduces kerfs taper but significantly increasing depth of cut, surface roughness.

They also conducted experiment by inversing the traverse direction but found that roughness increases. Finally, though 80° impact angle instead of 90°, increases depth of cut and surface quality marginally, but simultaneous settings of 80° impact angle with multiple passes, increases depth of cut rapidly. Stamdel et al proved that higher hardening of 34CrMo4 steel causes large declination angles on striation marks.

Higher tempering temperature causes carbides to coarsen and increases their volume ratio in steel structure a result inter-particles distances between carbides get reduced. Plastic deformation by means of a traverse slip mechanism can thus occur easily with very small effect of hardening. The modification of steel with higher Ni content displays a lower AWJ declination angle in comparison with the same steel in its basic chemical composition. Wang et al reported that axial velocity of both the fluid phase and particle phase reduced with increase of standoff distance and velocity distribution trends to smooth form parabolic shape, but the velocity amplitude of particle phase is smaller than fluid phase. Radial velocity of fluid phase increases within small distance from center line, then rapidly goes down to zero and finally increases to its maximum value. Radial velocity distribution of particle phase shows similar fashion with the only difference in velocity amplitude.

A different type of research was performed by Palleda it was concluded that material removal rate is getting increased with presence of chemically active liquids such as an acetone and phosphorie acid rather than plain water mixed slurry and reaches a maximum value with

polyacrylamide. Kerf taper was found almost nil in case of polymer addition to the water as spreading of jet reduced after releasing from nozzle type.

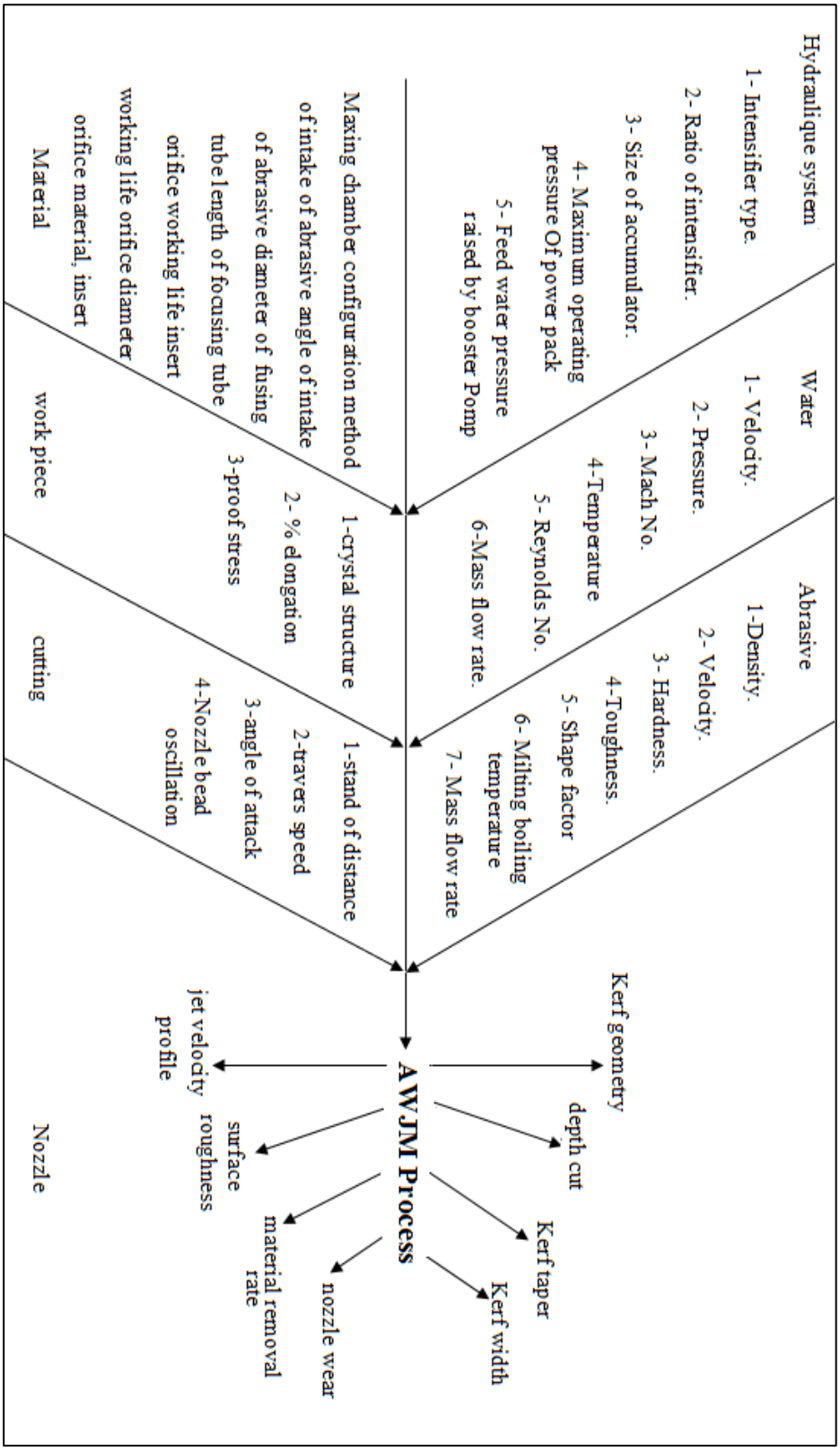

Figure II.3: *cause-effect diagram of AWJM process.*

II.6. Optimization:

From qualitative and quantities point of view, in any machining process optimum control parameter setting is still a challenging job the engineers. Optimum parameter setting can be found by discrete level search techniques. Using this method optimum levels are set for AWJM process among predefined levels used for experiments. Based fuzzy logic, simulated annealing and genetic algorithm are also applied for continuous searching operation between specified limits.

Different optimization techniques applied in different AWJM search work optimum control parameters setting within specified working range would always help the process engineers working more satisfactory. Chakrarthy et al proposed a GA based fuzzy logic optimized multi-criteria model for pradiso granite. Their optimized results predict depth of cut within 10% error. Kolhan et al applied simulated annealing for optimizing a regression model of depth of cut. Higher correlation coefficient (above 0.99) of they indicate the adequacy for particle use. **[5]**

Finally, comparing the results, integrated ANN-SA approach is found to be accurate than pure SA optimized model still optimum value of abrasive grit size differs in large with experimental findings. Later those researchers applied genetic algorithm on their own regression model. In that approach they reported that all the control parameters (including abrasive grit size) were validated with in very small error.

II.7. Conclusion:

A number of researchers work has already been done in AWJM process. Still exact understanding and also predicting of the outputs are not satisfactory. As AWJ works on any type of material so, versatile use of this process is always appreciated. Considering the conclusions drawn by several researchers, further study may be done in the following areas:

Based slicing, drilling, milling, AWJM may be used for boring operation. By precisely controlling the process parameters tolerance limit of whole dimension may be maintained at a very high level in boring. In case of turning, AWJ will remove the material rotating in the reverse direction (against conventional turning). As the small cutting force (impact force) act tangentially to the work piece, so chance of bending of work piece will be reduced.

Most of the researcher agreed that kerf taper formation and surface roughness can be reduced by oscillation the nozzle head into and fro direction. Cutting operation takes place horizontally. In case of structural application it may be required to move the jet vertically and gravitational action will play a vital role for controlling the jet.

Water behaves incompressible above the pressure 380 MPa. Simulated annealing, genetic algorithm, Taguchi's method were already applied for optimizing depth of cut, material removal rate and surface roughness in dividedly. Some more advanced optimization may be applied to get more accurate results. No such work is found regarding simultaneous optimization taking more than one responses at a time.

CHAPTRE III

Computational modeling

And method

III.1. Introduction:

We introduce basic properties of multiphase flows with dimensionless numbers used for characterizing the flow states. Based on the specifications of relevant multiphase flows, the chosen numerical modeling approach is explained. The decision of applying the Eulerian approach in the framework is likewise motivated. Building on the modeling approach, we introduce the basic governing equations and closures for momentum exchange and turbulence. In addition, we focus on turbulence modulation and different models are described. Finally, we explain the numerical simulation applied for handling and solving the problem that we studied, and some fundamental information on the employed CFD framework are also given.

III.1.1. Objective:

The objectives of the thesis have been set as follows:

- To simulate the water-air-solid with the AWJ nozzle application by Euleurian model in CFD program and to design the geometry of the nozzle, to investigate the 2D simulation with various inlet taper angle.
- By performing CFD simulation, to simulate three phase flow in the nozzle, to study the effects of different inlet angle on the exit velocity.

III.2. Multiphase flow theory:

Multiphase flow is flow with simultaneous presence of different phases, where phase refers to solid liquid or vapor state of matter there are four main categories of multiphase flows, gas-solid, liquid-solid and three phases flows, view **figure III.1**.

The definition of the flow regime is a description of the morphological arrangement of the components, or flow pattern **[8]**, the categorization of a multiphase flow in a certain flow regime is comparable to the importance of knowing if a flow is laminar or turbulent in single phase flow analyses **[9]**.

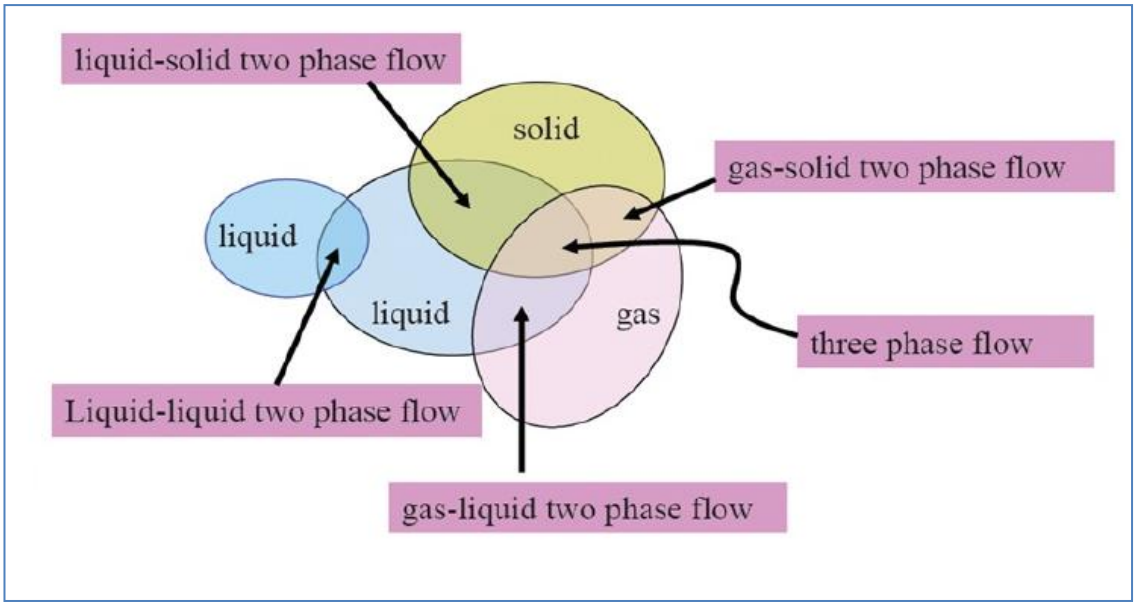

Figure III.8: *Multiphase flow regime.*

III.2.1. Numerical calculation of multiphase flow:

A multiphase flow model could be formed in terms of the local instant variables relating to each phase and matching boundary condition at all phases interfaces.

It is very complicate to obtain solution of multiphase directly or in another word it is almost impossible to solve directly. For the formulation of the multiphase flow, averaging procedures can be classified into three main groups, Ishii **[8]**; some of these modeling are presented below:

III.2.1.1. Euler-lagragian approach:

This approach is applicable to continuous dispersed systems and is often referred to as a discrete particle model or particle transport model. The primary phase is continuous and is composed of a gas or a liquid. The secondary phase is discrete and can be composed of particles drop or bubbles.

Conversation equations are solved for the continuous phase and the particle phase is tracked by solving the equation of motion for each particle see **equation III.1, III.2, III.3**.

$$\frac{\partial \alpha_f \rho_f}{\partial t} + \nabla \cdot \left(\alpha_f \times \rho_f \times u_f \right) = S_{mass} \qquad \text{(III.1)}$$

$$\frac{\partial \alpha_f \rho_f}{\partial t} + \nabla \cdot \left(\alpha_f \times \rho_f \times \bar{u}_f \right) = \alpha_f \nabla p - \alpha_f \nabla \cdot \tau_f - Sp + \alpha_f \rho_f g = 0 \qquad \text{(III.2)}$$

$$\frac{\partial Up}{\partial t} = \sum F \qquad \text{(III.3)}$$

Here α is volume fraction, S_{mass} is a mass source term existing in the case of exchange of mass between the phases, Sp momentum source term existing in case of exchange of momentum between the phases and F is force preferred to the fluid and particles phases, respectively.

The eulerian-lagragain is suitable to unit operation in with the volume fraction of the dispersed phase is small **[8]**.

III.2.1.2. Eulerian-Eulerian approach:

Eulerian-Eulerian is the most general approach for solving multiphase flows. It is based on the principle of interpenetrating continua, where each phase is governed by the Navier-Stockes equation; each phase is described by its physical properties and its own velocity, pressure, concentration and temperature field.

The Eulerian-Eulerian approach is applicable for continuous-dispersed and continuous systems. Since the volume of a phase cannot be occupied by the other phases.

The concept of volume fraction is introduced these volume fraction is assumed to be functions of space and time and their sum is equal to one conservation equations for each phase are derived to obtain a set of equations which have similar structure for all phases these equations are closed by providing constitutive relations that are obtained from empirical information. Euler-Euler approaches are relatively faster but require proper formulation of the constitutive equations. In FLUENT three different euler-euler multiphase models are available, they are:

- Volume of fluid method (VOF);
- Mixture model;
- Euleurian model.

III.2.1.2.1. Volume of fluid method:

The volume of fluid method is one of the most well known methods for volume tracking and locating the free surface. VOF belongs to the euler-euler framework where all phases are treated as continuous, and because the fluids do not mix, each computational cell is filled with purely one fluid and purely another fluid or the interface between two (or more)

fluids. The VOF method use a phase indicator function, sometimes also called a color function, to track the interface between two or more phases.

III.2.1.2.2. Mixture model:

The mixture model is designed for two or more phases (fluid or particulate). As in the Eulerian model, where the different phases move as at different velocities and also it is applicable to model homogeneous multiphase flow and to calculate non Newtonian viscosity. It can solve both the continuity equation and the momentum equation for the mixture, and the volume fraction equation for the secondary phases as well as algebraic expressions for the relative velocities.

III.2.1.2.3. Euleurian model:

An Eulerian multi-fluid model has been adopted where gas, liquid and solid phases are all treated as continua, interpenetrating and interacting with each other everywhere in the computational domain. The pressure field is assumed to be shared by all the three phases, in proportion to their volume fraction.

The motion of each phase is governed by respective mass and momentum conservation equation.

a) Continuityequation:

$$\frac{\partial(\varepsilon_k \rho_k)}{\partial t} + \nabla(\rho_k \varepsilon_k \bar{u}_k) = 0 \qquad \text{(III.4)}$$

Where ρ_k : the density; ε_k : the volume fraction of phase; K: gas, solid, liquid.

The volume fraction of the three phases satisfy the following condition:

$$\varepsilon_l + \varepsilon_g + \varepsilon_s = 1$$

b) Momentum equation: ***for liquid phase***

$$\frac{\partial(\rho_l \varepsilon_l \bar{u}_l)}{dt} + \nabla(\rho_l \varepsilon_l \bar{u}_l \bar{u}_l) = -\varepsilon_l \nabla P + \nabla\left(\varepsilon_l \mu_{eff}\left(\nabla \bar{u}_l + (\nabla \bar{u}_l)^T\right)\right) + \rho_l \varepsilon_l g + M_{i,L} \qquad \text{(III.5)}$$

c) Momentum equation: ***for gas phase***

$$\frac{\partial\left(\rho_g\,\varepsilon_g\,\bar{u}_g\right)}{dt}+\nabla\left(\rho_g\,\varepsilon_g\,\bar{u}_g\,\bar{u}_g\right)=-\varepsilon_g\,\nabla P+\nabla\left(\varepsilon_g\,\mu_{eff}\left(\nabla\bar{u}_g+\left(\nabla\bar{u}_g\right)^T\right)\right)+\rho_g\,\varepsilon_g\,\mathrm{g}+M_{i,g}\quad\text{(III.6)}$$

d) Momentum equation: ***for solid phase***

$$\frac{\partial\left(\rho_s\,\varepsilon_s\,\bar{u}_s\right)}{dt}+\nabla\left(\rho_s\,\varepsilon_s\,\bar{u}_s\,\bar{u}_s\right)=-\varepsilon_s\,\nabla P+\nabla\left(\varepsilon_s\,\mu_{eff}\left(\nabla\bar{u}_s+\left(\nabla\bar{u}_s\right)^T\right)\right)+\rho_s\,\varepsilon_s\,\mathrm{g}+M_{i,s}\quad\text{(III.7)}$$

Where P is the pressure and μ_{eff} is the effective viscosity. The terms $M_{i,l}$, $M_{i,g}$ and $M_{i,s}$ of the above momentum equations represent the inter-phase force term for liquid gas and solid phase, respectively.

III.3. Modeling approach:

The modeling of the abrasive water jet machining process is based on few important principles of fluid dynamics and fluid systems. They are Bernoulli's principle (**Fig.III.2**) intensifier and mixing chamber.

In fluid dynamics, Bernoulli's principle states that for an inviscid an increase in the speed of the fluid occurs simultaneously with a decrease in pressure or a decrease in the fluid's potential energy. The fundamental principle of the law of conservation of energy is used for an ideal fluid and is as follows:

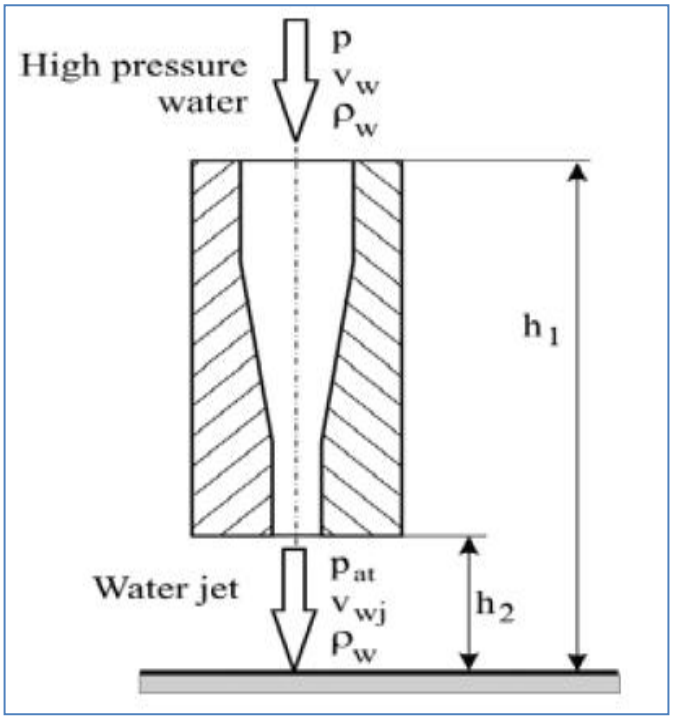

Figure III.2: *Bernoulli's theorem applied to water jet machining process.*

$$P + \frac{\rho_w V_w}{2} + \rho_w g h = const \quad \text{(III.8)}$$

Where, P: water pressure, V_w: velocity of water, ρ_w: density of water, g: acceleration due to gravity and h: height of the observed points above the reference plane.
By observing the leakage of high pressure water jets in the air and using equation (III.8), one can determine the leakage velocity of water jet from a nozzle based on water pressure.

In water jet machining, using direction control valve, the hydraulic unit drives the intensifier. Further, the water can be directly provided to the small cylinder of the intensifier. It can also be delivered through a pump known as booster pump. The pump then usually raises the pressure of the water to approximately 11 bar before delivering it to the intensifier. Thus, as the intensifier works, it delivers high pressure water. As the larger piston changes direction within the intensifier, there would be a drop in the delivery pressure. Cutting head consists of orifice, mixing chamber and focusing tube or insert where water jet is formed and mixed with abrasive particles to form abrasive water jet.

The velocity of the water jet thus formed can be estimated, assuming no losses as:

$$V_{wj} = \sqrt{\frac{2P}{\rho_w}} \quad \text{(III.9)}$$

Using Bernoulli's equation where, P is the water pressure and ρ_w is the density of water. The orifices are typically made of sapphire. In commercial machines, the life of the sapphire orifice is typically around 100 – 150 hours. In water jet machining, this high velocity water jet is used for the required application where as in abrasive water jet machining it is directed into the mixing chamber. the velocity of the water is very high and is issued from the orifice into the mixing chamber. As a result, a low pressure (vacuum) is created within the mixing chamber. By exploiting this principle and making use of the advantage, the metered abrasive particles are introduced into the mixing chamber through a port.

The abrasive particles are introduced within the water jet. Finally, because of this mixing action, the abrasive water jet comes out of the focusing tube as fully developed. It is evident that during the process of mixing, the abrasive particles are gradually accelerated. This is because of the transfer of momentum from the water phase to abrasive phase. Further, the jet lastly leaves the focusing tube, phases, water and abrasive, Abrasive particles during mixing try to enter the jet, but they are reflected away due to interplay drag force.

They go on interacting with the jet and the inner walls of the mixing tube, until they are accelerated using the momentum of the water jet considering the energy loss through water jet development at the orifice, the water jet velocity is estimated and obtained as given by the expression:

$$V_{wj} = \psi \sqrt{\frac{2P_w}{\rho_w}} \quad \text{(III.10)}$$

Where, ψ : Orifice parameter known as the coefficient of velocity. The volume flow rate of water may be expressed as:

$$q_W = \Phi \cdot V_{wj} \cdot A_{orifice} \quad \text{(III.11)}$$

Where, $A_{orifice}$ is the area of the orifice, given by:

$$A_{orifice} = \frac{\pi}{4} d_{0\,orifice}^2 \quad \text{(III.12)}$$

III.4. Computational fluid dynamic:

CFD is the science of predicting fluid flow, heat transfer, chemical reactions, and related phenomena by solving the mathematical equations which govern these processes using a numerical process. Bakker**[18]**said that CFD is one of the branches of fluid mechanisms that uses numerical methods and algorithms to solve and analyze problems that involve fluid flow.

The fundamental basis of any CFD problem is the Navier-Stokes equations which define any single-phase fluid flow these equations can be simplified by removing terms describing viscosity to yield the Euler equations. It uses numerical methods to solve these fundamental nonlinear differential equations for pre-defined geometries and boundary conditions to linearized form.

The result of CFD is relevant engineering data which are used in conceptual studies of new design, Anderson**[19]**. The various general CFD packages is PHONICS, CFX, FLUENT, FLOW3D and STAR-CD, most of this programs are based on the finite volume method and are used to solve fluid flow and heat and mass transfer problem.

III.4.1. Working of CFD code:

Fluid dynamics is the science of fluid motion. Fluid flow is commonly studied in one of three ways:

- Experimental fluid dynamics

- Theoretical fluid dynamics
- Numerically: computational fluid dynamics (CFD)

CFD is one of the branches of fluid mechanics **[24]**. It is the science of predicting fluid flow, heat transfer, mass transfer, chemical reactions, and related phenomena by solving the mathematical equations which govern these processes using numerical methods and algorithms. In order to provide easy access to their solving power all commercial CFD packages include sophisticated user interfaces to input problem parameters and to examine the results. Hence all CFD codes contain three main elements:

1. **Pre-processor:** pre-processing consists of the input of a flow problem to a CFD program by means of an operator-friendly interface and the subsequent transformation of this input into a form suitable for use by the solver **[31]**. The region of fluid to be analyzed is called the computational domain and it is made up of a number of discrete elements called the mesh (or grid). The users need to define the properties of fluid acting on the domain before the analysis is begun; these include external constraints or boundary conditions, like pressure and velocity to implement realistic situations.
2. **Solver:** a program that calculates the solution of the CFD problem. Here the governing equations are solved. This is usually done iteratively to compute the flow parameters of the fluid as time elapses. Convergence is important to produce an accurate solution of the partial differential equations.
3. **Post-processor**: used to visualize and quantitatively process the results from the solver. In a contemporary CFD package, the analyzed flow phenomena can be presented in vector plots or contour plots to display the trends of velocity, pressure, kinetic energy and other properties of the flow.

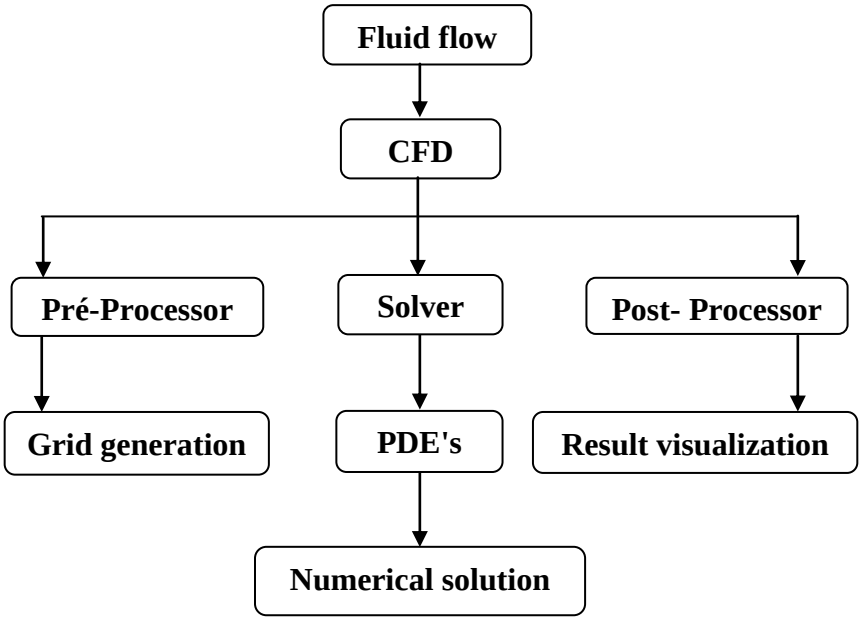

Figure III.9: *Overview of CFD* ***[18].***

III.4.2. Mathematical formulation:

III.4.2.1. Finite difference method FDM:

The FDM employs the concept of Taylor expansion to solve the second order partial differential equations (PDE) in the governing equations of fluid flow. It's the oldest model, the basic of this model or method consists in the field of meshing studies to give an approximation of the contour of the domain by applying an easy algebraic equation.

III.4.2.2. Finite element method FEM:

Is based largely on the basic finite element procedures used: The formulation of the problem invariational form, the finite element discretization of this formulation, and the effective solution of the resulting finite element equations.

These basic steps are the same whichever problem is considered and together with the use of the digital computer present a quite natural approach to engineering analysis in the meshing. The mesh can be made up to triangle or rectangles whose vertices are looking for volumes of the unknown.

III.4.2.3. Finite volume method FVM:

The finite volume method is a numerical technique that transforms the partial deferential equations representing conservation laws over differential volumes into discrete algebraic equations over finite volumes, Moukalled et al **[32]**. The finite volume method is characterized

by its advantage in satisfying mass, momentum and energy conservation in all finite volumes as well as in the entire computational domain.

In 2D, one could also have triangular cells. In 3D, cells are usually hexahedrals, tetrahedrals, or prisms. In the finite-volume approach, the integral form of the conservation equations are applied to the control volume defined by a cell to get the discrete equations for the cell. The integral form of the continuity equation for steady, incompressible flow is:

$$\int_S \bar{V} \cdot n \cdot dS = 0 \qquad \text{(III.14)}$$

The integration is over the surface *S* of the control volume and n is the outward normal at the surface. Physically, this equation means that the net volume flow into the control volume is zero. The continuity equation and the momentum equation, also known as the Navier-Stockes equation, are needed and used generally to solve any state of flow in CFD modeling; in addition there are the energy equation and mass conservation that maybe needed to describe a nature of particular flow.

1. Conservation of mass:

Let $\rho(x,t)$ be the density of a fluid at a point x at time t, let $u(x,t)$ be its velocity. Let Ω be the domain occupied by the fluid and O a regular sub-domain of .To conserve the mass, the rate of change of mass of the fluid in $O, \frac{\partial(O\rho)}{\partial t}$, has to be equal to the mass flow across the boundary **[27]**:

$$\int \nabla \cdot u = \int v \cdot n \qquad \text{(III.15)}$$

And the fact that O is arbitrary we get immediately the equation of conservation of mass.

$$\rho,t + \nabla \cdot (\rho U) = 0 \qquad \text{(III.16)}$$

2. Conservation of momentum:

The principle of conservation of momentum makes it possible to establish the relations between the characteristics of the fluid and its movement and the reason that produce it. This equation can be written in the following explicit form:

- According to the x-axis:

$$u\frac{\partial u}{\partial x}+v\frac{\partial u}{\partial y}=-\frac{1}{\rho}\frac{\partial p}{\partial x}+v\left(\frac{\partial u^{2}}{\partial x^{2}}+\frac{\partial u^{2}}{\partial y^{2}}\right) \quad \text{(III.17)}$$

- According to the y-axis:

$$u\frac{\partial v}{\partial x}+v\frac{\partial v}{\partial y}=-\frac{1}{\rho}\frac{\partial p}{\partial y}+v\left(\frac{\partial v^{2}}{\partial x^{2}}+\frac{\partial v^{2}}{\partial y^{2}}\right) \quad \text{(III.18)}$$

3. Conservation of energy:

Lastly, an equation called conservation of energy can be obtained by writing the total energy of a volume element $O(t)$ moving with the fluid. The equation can be obtained by the first principal of thermodynamics; this principal relates the different forms of energy. It's obtained by:

$$\nabla\cdot\left(\rho\cup T\right)=\nabla\cdot\left(\frac{\lambda}{Cp}\cdot\nabla T\right) \quad \text{(III.19)}$$

Or:

$$u\frac{\partial u}{\partial x}+v\frac{\partial u}{\partial y}=a\left(\frac{\partial T^{2}}{\partial x^{2}}+\frac{\partial^{2}x}{\partial^{2}y}\right) \quad \text{(III.20)}$$

We note that the energy of a volume element O is the sum of potential energy and the kinetic energy $\rho\frac{x\,v^{2}}{2}$.

III.4.3. Presentation of gambit and fluent:

Numerical flow simulation software based on the volume method finished products can now be regarded as true "digital experiments", the advantage of "numerical methods" is that all physical quantities related to the flow (velocity field, pressure field, stresses etc) are immediately available at any point in the flow. The resolution of fluent flow simulation soft ware requires presentation of software GAMBIT or another mesh.

III.4.3.1. Gambit:

Gambit is a CAD computer aid design and mesh creation it allow us to create a 2d or 3d geometries and build a mesh for it.

It also used to all the difficult and hard design and it's use is not very hard mostly consist of the mouse, it's widely famous in the industry because of its powerful graphical interface.

When you start gambit, either in the batch mode or in the real-time mode employing the GUI, GAMBIT creates a modeling session, it consist of all operations performed in relation to a Gambit mode**[34]**:

- Import of geometry and mesh information.
- Creation of geometry.
- Creation and refinement of a mesh.
- Assignment of zone types.
- Creation and modification of coordinate systems and grids.
- Changing the appearance and orientation of the model as displayed in the graphics windows.

a. Mesh:

The calculation code "FLUENT" in version 6.2 treats several types of structured, unstructured or hybrid meshes. A structured mesh is usually composed of quadrilateral meshes in two dimensions (2D or surface mesh) and hexahedral three-dimensional (3D or volumetric mesh), while an unstructured mesh will be composed of quadrilateral or triangular meshes in 2D and hexahedral Or 3D tetrahedrons. In a hybrid mesh, the meshes close to the walls are quadrilaterals in 2D and hexahedrons in 3D and the meshes of the rest of the domain are 2D triangles and 3D tetrahedrons.

In close proximity, it is necessary to have the smallest meshes possible to model the flows at this place, this particularity is all the more important in turbulent regime, it is called (inflation). In 3D, the meshes that make the connections between the hexahedra and the tetrahedrons are prisms or pyramids.

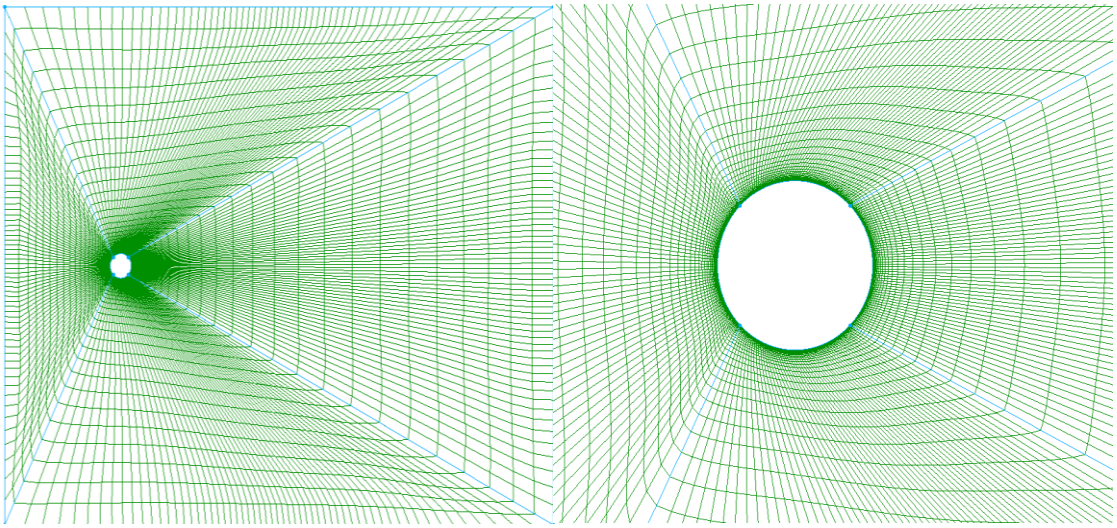

Figure III.4: *view of different meshes.*

III.4.3.2.FLUENT:

FLUENT is a computational code for modeling fluid flows and heat transfer in complex geometries. It can solve flow problems with unstructured meshes, which can be produced for complex geometries, with relative ease.

FLUENT uses the finite volume method as a method of discrediting the equations that govern flow, such as the equation of continuity and momentum and energy. Using this technique based on the integration of equations on a control volume, "FLUENT" goes through the following steps:

✓ *Division of the domain into discrete control volumes using a calculation grid (meshing);*

✓ *Integration of the governing equations on the individual control volumes, in order to construct the algebraic equations for the discrete dependent variables, the unknowns such as velocities, pressures and temperatures;*

✓ *Linearization of the discretized equations and solution of the system of linear equations resulting, to account for the turbulent effects.*

III.4.3.3. Boundary condition:

For Fluent code the available types of boundary conditions are classified as follows:

a) ***Inlet and outlet flow conditions***: inlet pressure, Velocity inlet, mass flow inlet, intake, outlet pressure; Outflow, far-field pressure, exhaust.

b) ***Wall and conditions of the pole*****:** wall (wall), axis of symmetry (axis), periodic conditions, plane of symmetry (symmetry).

c) ***Cells of internal zones:*** fluid or solid (of different type).

d) ***Condition of the internal faces:*** ventilation, radiation, internal wall. But if we speak in a more general way we will have four types of boundary conditions or each one requires a thorough study:

- ***at the entry of the domain:*** *the value of the variable is known.*
- ***at the output of the domain:*** *either by knowing the value of the given variable or assuming that the regime is established*

III.4.3.4. Turbulence model:

The choice of turbulence model will depend on consideration such as the physics encompassed in the flow, the established practice for specific class of problem the level of accuracy required, the available computational resources, and the amount of time available for the simulation. In present simulation the standard K-ε model has been taken for turbulence modeling.

The standard K-ε model is a semi-empirical model based on model transport equations for the turbulence kinetic energy (K) and it's dissipation rate (E).The model transport equation for turbulence kinetic energy is derived from the exact equation while the model transport equation for dissipation rate has been obtained using physical reasoning and bears little resemblance to its mathematically exact counterpart from the following transport equation:

$$\frac{\partial}{\partial t}(\rho_k)+\frac{\partial}{\partial x_i}(\rho_k v_i)=\frac{\partial}{\partial x_j}\left[\left(\mu+\frac{\mu_t}{\sigma_k}\right)\frac{\partial k}{\partial x_i}\right]+G_k+G_b-\rho\varepsilon-YM+SK \qquad \text{(III.21)}$$

And

$$\frac{\partial}{\partial t}(\rho_\varepsilon)+\frac{\partial}{\partial x_i}(\rho_\varepsilon v_i)=\frac{\partial}{\partial x_j}\left[\left(\mu+\frac{\mu_t}{\sigma_\varepsilon}\right)\frac{\partial \varepsilon}{\partial x_i}\right]+C_{1\varepsilon}\frac{\varepsilon}{k}(G_k+C_{3\varepsilon}G_b)-C_{2\varepsilon}\rho\frac{\varepsilon^2}{K}+S\varepsilon \qquad \text{(III.22)}$$

The turbulence viscosity, (μ_t) is computed by combining K and ε as follows:

$$\mu_t=\rho C\mu\frac{K^2}{\varepsilon} \qquad \text{(III.23)}$$

III.5. Simulation approach:

Abrasive water jet is associated with highly turbulent flow. To predict the velocity distribution at the nozzle exit, water, air and solid slurry needs to be treated as a multi-phase

system. The simulations are carried out for steady state, turbulent flow with heat transfer. Water was considered as the primary phase. Simulations were made with k-ε turbulence model (turbulent kinetic energy and energy dissipation) using the CFD program.

III.5.1.Equations of the Simulations

The three phases were labeled by Greek indices α, β and γ representing water, air and solid respectively and N_p denotes the number of phases. The volume fraction of each phase is denoted by r_α. Governing equations were solved for the time averaged values of the velocity components, pressure, volume fractions and turbulence parameters. The equations were closed using k-εturbulence model. The equations are presented below. Hence the subscript α denotes the phase water. Equations for air and solid phases can be obtained by replacing α with β and γ respectively **[34]**.

a) The continuity equation:

$$\nabla \cdot \left(r_\alpha \rho_\alpha U_\alpha \right) = 0 \qquad \text{(III.24)}$$

b) The momentum equation:

$$\nabla \cdot \left(r_\alpha \left(\rho_\alpha U_\alpha - \mu_{\alpha eff} \left(\nabla U_\alpha + \left(\nabla U_\alpha \right)^T \right) \right) \right) = r_\alpha \left(B - \nabla p_\alpha \right) + \sum_{\beta=1}^{N_p} c_{\alpha\beta}^{(d)} \left(U_\alpha - U_\beta \right) + F_\alpha \qquad \text{(III.25)}$$

$c_{\alpha\beta}^{(d)}$ is the inter-phase drag term between phase α (water) and phase β (air) where:

$$\mu_{\alpha\,\mathrm{eff}} = \mu_\alpha + \mu_{\mathrm{T}\alpha} \qquad \text{(III.26)}$$

$\mu_{\alpha\,\mathrm{eff}}$ is the effective viscosity, μ_α is the molecular viscosity and $\mu_{\mathrm{T}\alpha}$ is the turbulent viscosity (equation III.23).

c) The energy equation:

$$\nabla \cdot \left(r_\alpha \left(\rho_\alpha U_\alpha H_\alpha - \lambda_\alpha \nabla T_\alpha \right) \right) = \sum_{\beta=1}^{N_p} c_{\alpha\beta}^{(h)} \left(T_\beta - T_\alpha \right) \qquad \text{(III.27)}$$

Where H_α is the static enthalpy, $H_\alpha = h_\alpha \left(T_\alpha \right)$, $c_{\alpha\beta}^{(h)}$ is the inter-phase heat transfer term.So the constitutive equation for each phase is as follow:

$$h_\alpha = h_\alpha \left(T_\alpha P_\alpha \right) \qquad \text{(III.28)}$$

Considering that the volume fraction sum is unity:

$$\sum_{\alpha=1}^{Np} r_\alpha = 1 \qquad \text{(III.29)}$$

The general advection-diffusion equation is:

$$\nabla \cdot \left(r_\alpha \left(\rho_\alpha U_\alpha \Phi_\alpha - \Gamma_\alpha \nabla \Phi_\alpha \right) \right) = r_\alpha S_\alpha + \sum_{\beta=1}^{N_p} c_{\alpha\beta} \left(\Phi_\beta - \Phi_\alpha \right) \qquad \text{(III.30)}$$

d) Equation of volume fraction:

$$\nabla \cdot \left(r_\alpha \rho_\alpha U_\alpha - \Gamma_\alpha \nabla r_\alpha \right) = 0 \qquad \text{(III.31)}$$

e) The transport equation for K-ε turbulence model :

$$\nabla \cdot \left(r_\alpha \left(\rho_\alpha U_\alpha \varepsilon_\alpha - \left(\mu + \frac{\mu_{T\alpha}}{\sigma_\varepsilon} \right) \nabla \varepsilon_\alpha \right) \right) = r_\alpha S_{\varepsilon\alpha} + \sum_{\beta=1}^{N_p} c_{\alpha\beta}^{(\varepsilon)} \left(\varepsilon_\beta - \varepsilon_\alpha \right) \qquad \text{(III.32)}$$

Since air was considered as compressible flow, its density will then change with changes in pressure and temperature.

III.6. Conclusion:

Several error sources exist for numerical simulations. Numerical approximation errors will always occur but another error source, which often is difficult to detect, is usage error. Unintended application of models, badly chosen parameters or wrongfully applied boundary conditions can lead to unphysical and inaccurate results. With the extended use of CFD simulations in engineering work it is of high importance to investigate the accuracy of commercial codes as well as understanding the choice of models. This is particularly important for multiphase flow where the complexity of both physical laws and numerical treatment makes the development of general models difficult**.**

Chapter IV

SIMULATION AND INTERPRETATION OF RESULT

IV.1. Introduction:

In the present work of three phases water-air-solid (abrasive beads) which are initially in residual condition inside the nozzle. The water, liquid phase and air are introduced at the start. The model's equations described in chapter **III** are solved using the commercial CFD software package **FLUENT 6.3.26**; **figure IV.1** shows the general procedure for the simulation using **FLUENT** software. The simulation will be based on an experimental study that zoltani**[35]** and Dewan et al **[34]** did, to enable validation of the results, the finding of the model survey and simulations will result in general recommendations for multiphase CFD simulations including guidance on the effect of choice of model, setting…etc. In this work, Eulerian model have been chosen to simulate three phases flow in AWJ nozzle, we have used a steady approach for all simulation.

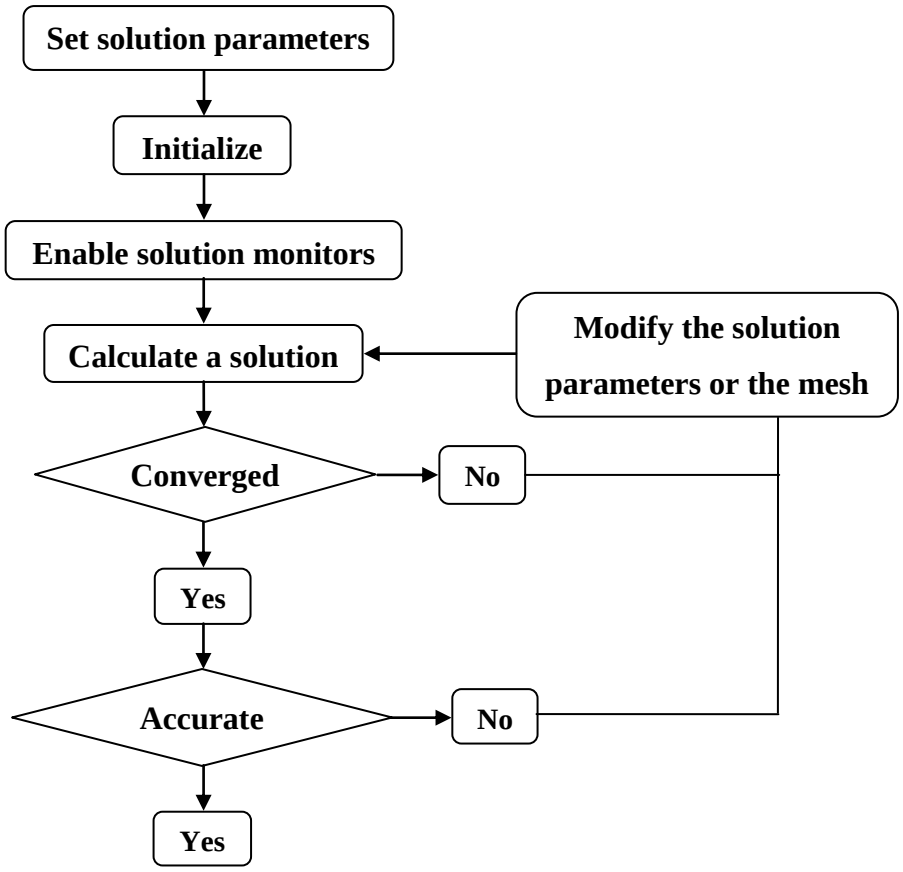

Figure IV.1: *Flow chart showing the general procedure for the simulation using FLUENT.*

IV.2. Geometry and mesh:

The first step in CFD simulation of AWJ nozzle which has been done by GAMBIT tools to design the problem in geometrical configuration and mesh the geometry. Before fluid flow

problems can be solved, FLUENT needs the domain in which the flow takes place to evaluate the solution.

The flow domains as well as the grid generation into the specific domain have been created in GAMBIT; four domains were created with dimensions taken from the study of Dewan et al **[34]**. For all four domains the inner diameter of the mixing chamber was 6mm, for the orifice the diameter was 0.33mm, and the length of the mixing chamber was taken $Lc = 12\,mm$. For the focus tube we took a diameter $df = 1.27\,mm$ and a length of 75mm. lastly the diameter of the abrasive inlet we took a dimension of 3mm, for the taper inlet angle was changed from 45° to 82°, respectively. The air and water and solid were taken as a continua phase, for the grid that has been created in GAMBIT which is shown in **figure IV.2**. Gambit has been used to create the geometry of the nozzle with desired dimensions, we have created a two dimensional geometry, for three phase flow (water, air, solid) the surrounding was considered to be in atmospheric condition.

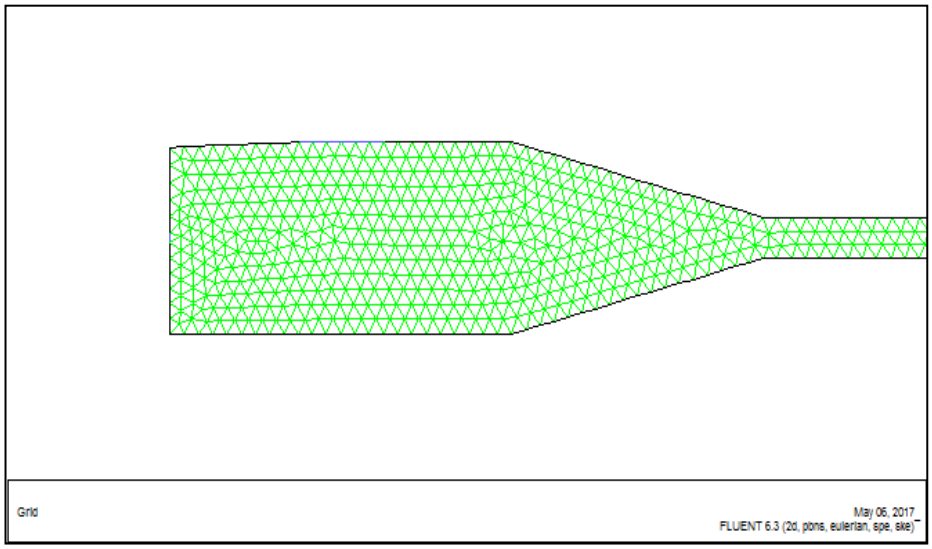

Figure IV.2: *tetrahedral meshing of AWJ nozzle.*

IV.3. Boundary and initial condition:

In order to obtain a well-posed system of equations, reasonable boundary conditions for the computational domain have to be implemented for our simulation we had two inlets.

The inlet pressure and flow rate for the air and liquid phase were not known from the experimental study. For the outlets, we didn't have any information or was mentioned in the paper of Dewan et al **[34].** However, for some simulations a pressure outlet condition had to be implemented to achieve convergence as the pressure outlet condition is more stable than

the flow split condition. The values for the outlet pressures were then taken from a previously converged simulation and adjusted to obtain the correct bulk flow split.

Additional boundary conditions had to be specified when modeling was implemented. Using the CFD model, a value for the interfacial area concentration at the inlet had to be specified. The default value in Fluent was used. In the first inlet boundary condition is a uniform liquid pressure which was set as 276 MPa. For the secondary inlet a mass flow boundary condition was established for the abrasive and air inlet we took 0.45Kg/min and flow rate of 2.67 lit/min respectively.

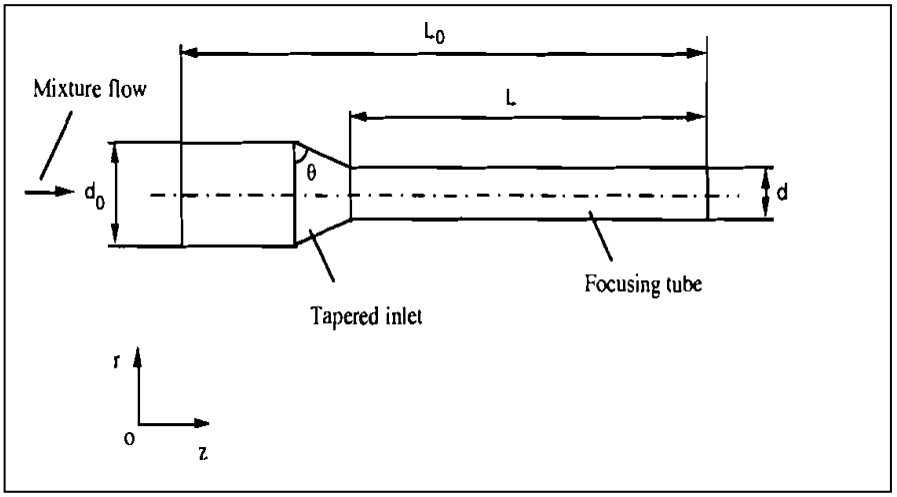

Figure IV.3: *schematic diagram of AWJ nozzle* ***[36].***

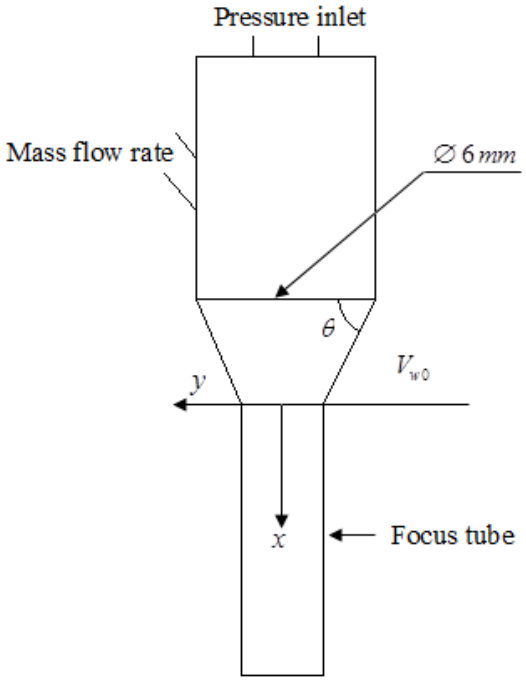

Figure IV.4: *Schematic diagram show the boundary condition used.*

We can calculate the value of V_{w0} by using the Bernoulli equation that was used by Abduka et Nadeau **[30]**:

$$v_{w0} = \sqrt{\frac{2P}{\rho_{water}}} \qquad \text{(IV.1)}$$

$$v_{w0} = \sqrt{\frac{2(276.10^6)}{1000}} = 742.96 \text{m/s} \quad \text{for} \quad x = 0$$

For the initial boundary condition view **table IV.1**and **table IV.2** for the type of the boundary that we took in our study:

Physical and process parameters	Geometry
Diameter of abrasive	180µm
Density of solid	4100Kg/min
Mass flow of solid	0.45 Kg/min
Water density	1000 Kg/min
Water pressure	276MPa
Air flow rate	2.67 Lit/min
Air pressure	0.76 MPa
Air density	1.29Kg/min

Table IV.5: *The inlet boundary condition* ***[34]***

Zone	Type of boundary
Inlet 01	Pressure inlet
Inlet 02	Mass flow rate
Wall	Wall
Outlet	Pressure outlet

Table IV.6: *The boundary condition type.*

IV.4. Simulation setup:

A commercial CFD package **ANSYS FLUENT 6.3.26** is used for the numerical solution of the flow, this CFD code is based on a finite volume approach; in this section the various CFD code settings and options are summarized. For all cases, steady and pressure based solver

are used, the euler-euler method based on a three phases system is employed with a K-ε model for the turbulence.

The pressure, velocity coupling is obtained using the phase coupled **SIMPLE algorithm**, the simulation setting is shown in **table IV.3**:

Settings	**Choice**
Simulation type	2D, steady
Solver	pressure based and implicit
Temporal discretization	1st order
Multiphase model	Eulerian, 3 phase, implicit
Turbulence model	k-ε, mixture model
Pressure-velocity coupling	Phase coupled SIMPLE
Momentum	1st order upwind
Volume fraction	1st order up wind
Turbulent kinetic energy	1st order upwind
Turbulent dissipation rate.	1st order upwind

Table IV.7: *simulation settings.*

The solution procedure involves the following steps:

1. *Generation of suitable grid system;*
2. *Conversion of governing equation into algebraic equations;*
3. *Selection of discretization schemes;*
4. *Formulation of the discretized equation at every grid location;*
5. *Formulation of pressure equation;*
6. *Development of suitable iteration scheme for obtaining a final solution.*

The solution has been initialized from all zones, the convergence criteria are preset condition for the residuals that determine when an iterative solution is converged for any set of convergence criteria, the assumption is that the solution is no longer changing with more iteration and when the condition is reached there is an overall mass balance throughout the domain, the residual plot of progress is shown below in **figure IV.4**.

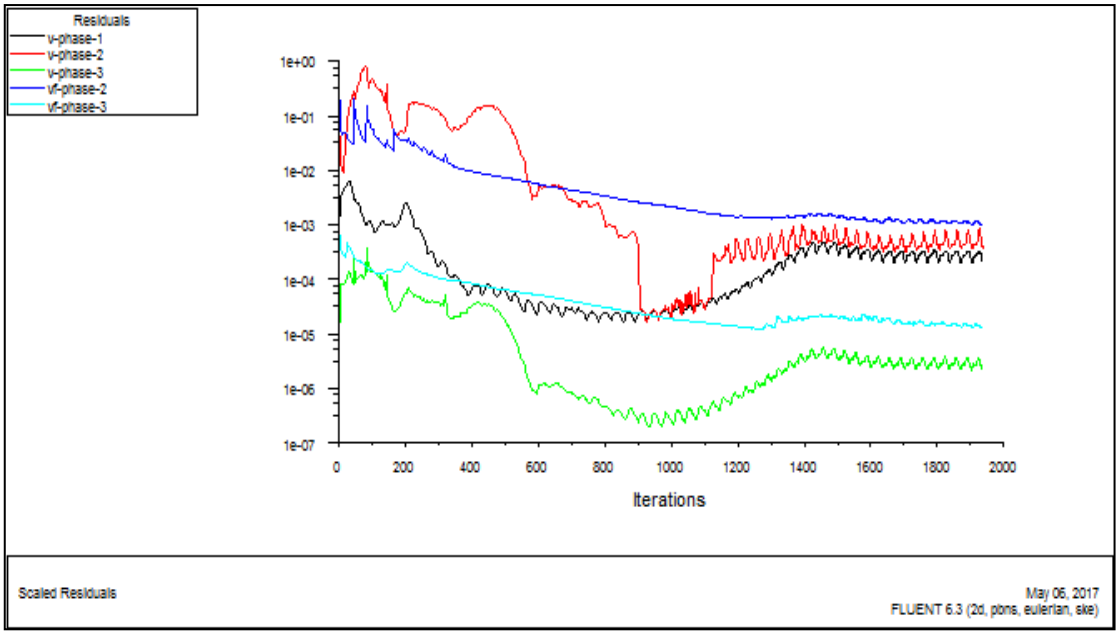

Figure IV.5: *Plot of residual proceeding with iteration for simulation in FLUENT.*

IV.5. Result and discussion:

In this section, the results from the simulations are presented and compared with experimental data. In the first section we presented the validation of our result that our thesis was based on and compared it with the experimental data, in section IV.5.2, we presented a some addition work that verify that our code did march.

IV.5.1.Different taper angle:

The numerical simulations carried out to find out the effect of taper inlet angle in abrasive water jet are presented here in the form of velocities of different phases at the exit. Results presented in **figure IV.6** clearly show that the taper inlet angle has influence on jet velocity at the exit of the focus tube.

Andreas Momber **[1]** showed that a certain acceleration distance in the tapered region of the mixing chamber is necessary to accelerate the injected particles. When the taper inlet angle is small there are more collisions between the phases and the wall, in the tapered zone. So, at the smaller taper inlet angles the velocities at the outlet were low. In the case of larger taper inlet angles the particles are accelerated but with the increase of total travel length there are more chances of collisions with the wall. In **figure IV.6** it indicates that the jet speed reaches a maximum at an optimum taper inlet angle of 75°. This substantial increase in length results in

more collision between the phases and also with the wall, leading to lower velocity at the exit at 82°.

Although the simulation was developed for three phases, it was very difficult to simulate the velocity of the three phases in order to fully validate the theoretical result. However, the velocity distribution at the exit of the focus tube was verified with experimental data for a three phase flow published by Dewan **[34]**.

In our study we did the simulation with Euleurian model because in the article they didn't mentioned the model that they used so we had to chose a model by our self despite that the Eulerian model is the hard model but we did our best to get an approaches result to what Dewan**[34]** found.

The result was approach in some angle but for some it went very far as we see in **figure IV.6**in the taper angle 75° we find that the velocity water go very high compared to Dewan**[34]** study. we don't know the reason but maybe because of the volume fraction that we wasn't sure about, because there wasn't any information talking about it in the article but the increase and decrease of velocity happened exactly at the same angle and as we see in the angle of 82° the velocity started to decrease. In the angle of 60° there was a really close result between our study and Dewan **[34]**, **Figure IV.6** show the diagram of our result.

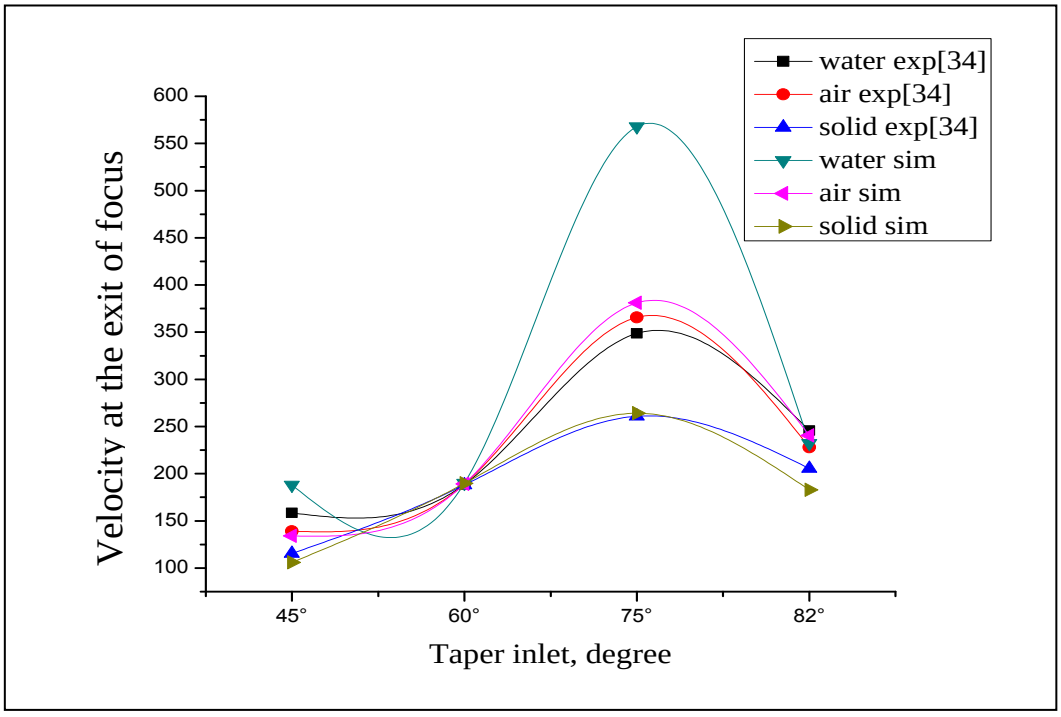

Figure IV.6: *Average exit velocities of different phases for different taper inlet angle.*

IV.5.1.1. Comparison:

In this section we will calculate the error between the experimental study and our simulation the percent difference is a comparison between a theoretical estimate and an experimental result. In most experiments instructions require you to calculate a theoretical value given certain initial conditions. This usually involves a mathematical treatment of an accepted theory. The experimental result is obtained by performing an experiment and recording a measurement. We can compare the experimental and theoretical values using the equation below:

$$\text{error } \% = \left|100\,(\text{numerical} - \text{theorical})\right| \;/\; \text{numerical} \qquad \text{(IV.2)}$$

a) Air phase:

	Degree	Numerical coordinate V [m/s]	Modified model (Simulation) V[m/s]	Error %
1	45°	138.88	134	3.51%
2	60°	188.88	189.13	0.13%
3	75°	365.72	381	4.17%
4	82°	228	240.43	4.31%

Table IV.8: *Comparison between the two result for air phase.*

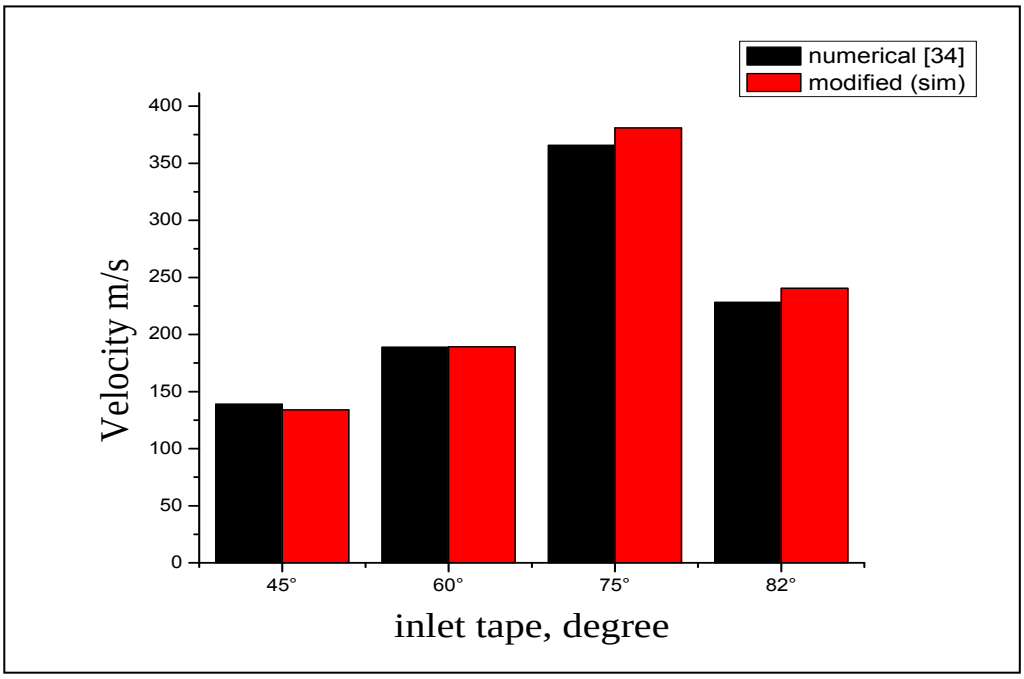

Figure IV.7: *Histogram for the results of air velocity.*

We can see in **table IV.4** the numerical coordinate that Dewan**[34]**, found in his simulation and in the second part it's the result and coordination that we found in our simulation that result include just one phase and it's the air phase. We calculated the error between the two result and as we see there were very close from each other, we can see that in 60° we only had a 0.13% error and that not a lot in the 75° and 82° each of them had 4.17%,4.31%, respectively so in fact that result tell us that our result in correct and that it's reasonable and that mean that we had validate our result the hexagram shows the error and how close the two result are in each angle.

b) Solid phase:

	Degree	Numerical coordinate V [m/s]	Modified model (Simulation) V[m/s]	Error %
1	45°	115.4	106	8.14%
2	60°	188.174	189.75	0.83%
3	75°	260.81	264	1.20%
4	82°	205.42	183	10.73%

Table IV.9: *Comparison between the two result for solid phase.*

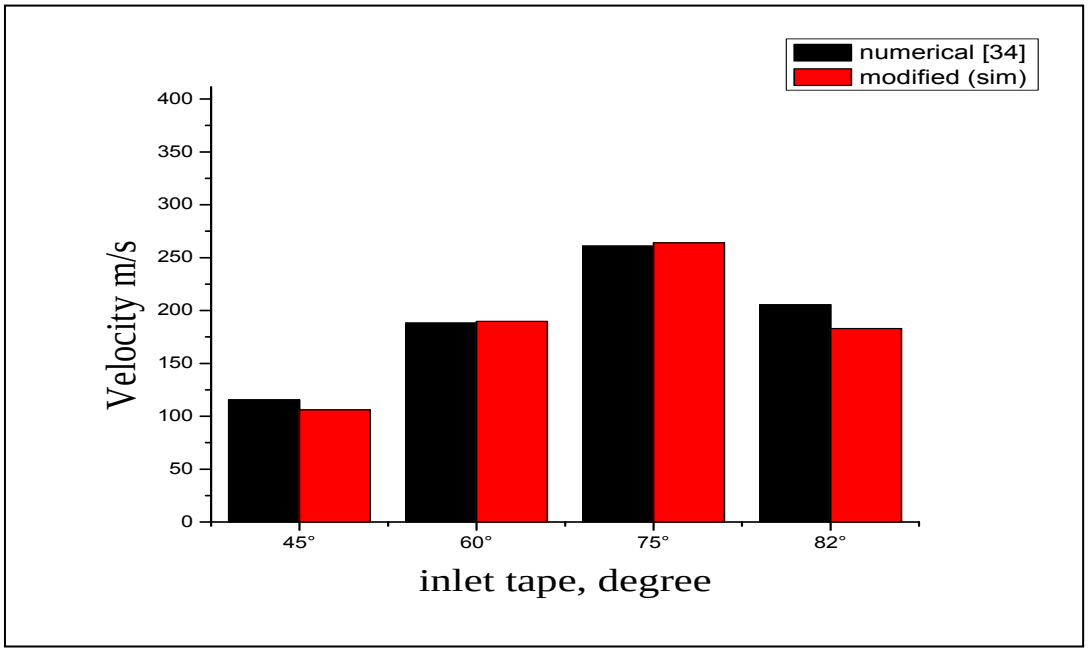

Figure IV.8: *Histogram for the results of solid velocity.*

We can see in **table IV.5** the numerical coordinate that Dewan**[34]**, found in his simulation and in the second part it's the result and coordination that we found in our simulation that result include just one phase and it's the solid phase. We calculated the error

between the two results and as we see there were very close from each other, we can see that in 60° we only had a 0.83% error and that not a lot in the 75° and 82° each of them had 1.20%, 10.63%, respectively and it was 8.41% for 45°.

c) Water phase:

	Degree	Numerical coordinate V [m/s]	Modified model (Simulation) V[m/s]	Error %
1	45°	158.571	188	18.55%
2	60°	188.571	189.97	0.74%
3	75°	348.57	568	56.29%
4	82°	245.714	232.227	5.48%

Table IV.10: *Comparison between the two result for water phase.*

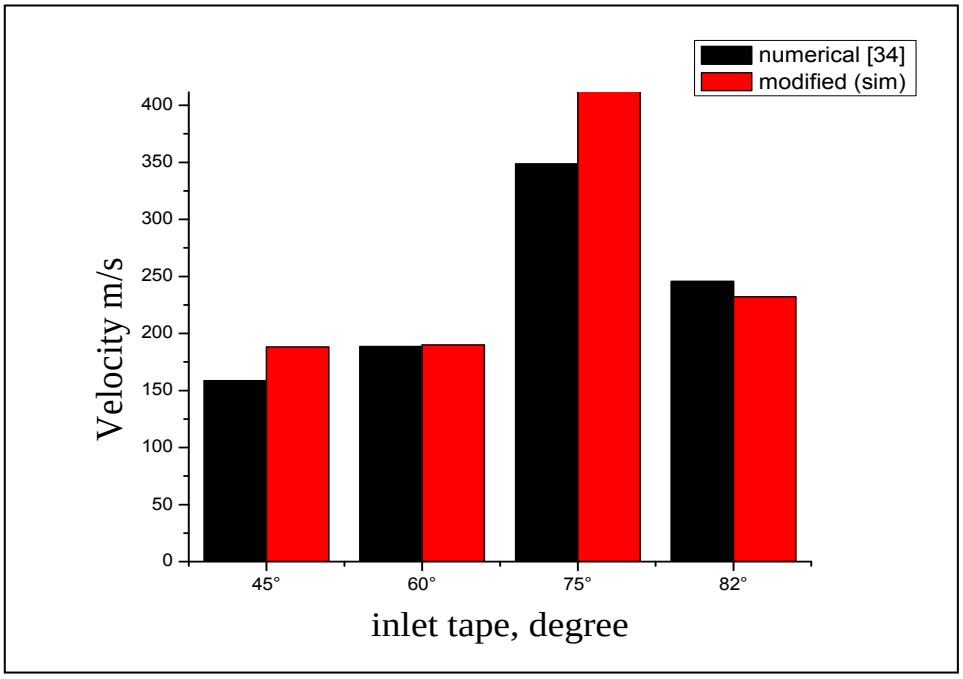

Figure IV.9: *Histogram for the result of water velocity.*

Finally, **table IV.6** shows the result that we got in water phase. We calculated the error between the two result and as we see there were very close from each other, we can see that in 60° we only had a 0.74% error and that not a lot in the 75° we had a hug error that was 56.29% maybe because of particle size so we can see that in our result the velocity of water at the outlet was increased hugely compared to Dewan result but because the two phases were

very close we just took the result as it is; the hexagram shows the error that we calculated already in the table and shows the distance between each result.

IV.5.2. the velocity outlet of the mixture:

There are few experiments done to find out the velocity distributions at the exit of the focus tube. The present numerical results were carried out by using Euleurian model and it shows the result that we got in our simulation **figure IV.10** shows the velocity obtained in the outlet for mixture.

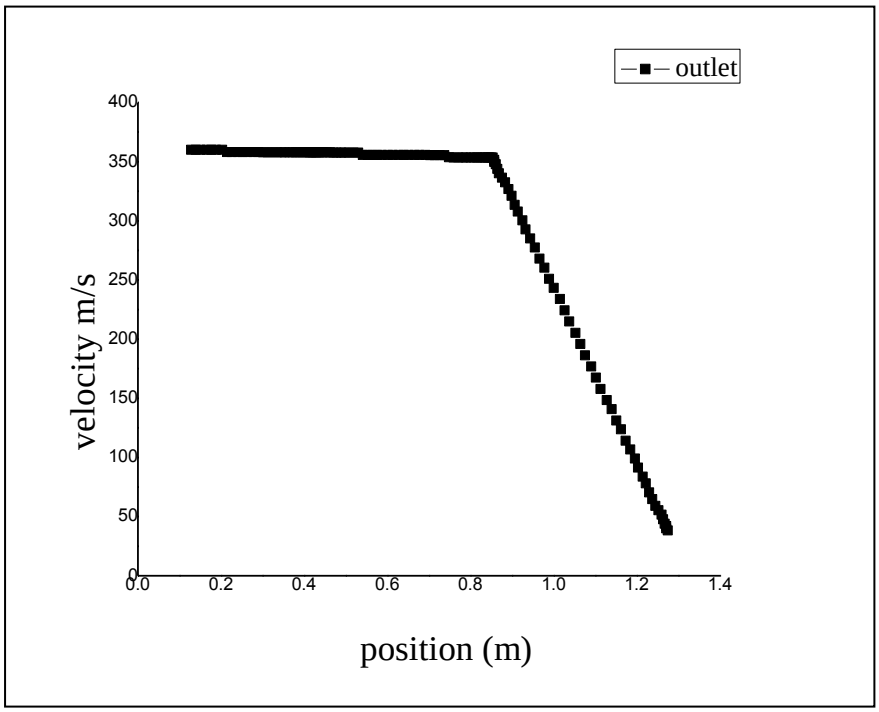

Figure IV.10: *plot of velocity obtained at the outlet.*

IV.5.3.Volume fractions:

Those three figures (**figure IV.11 to figure IV.13**) shows the changes that happen in volume fraction for each phase trough the simulation

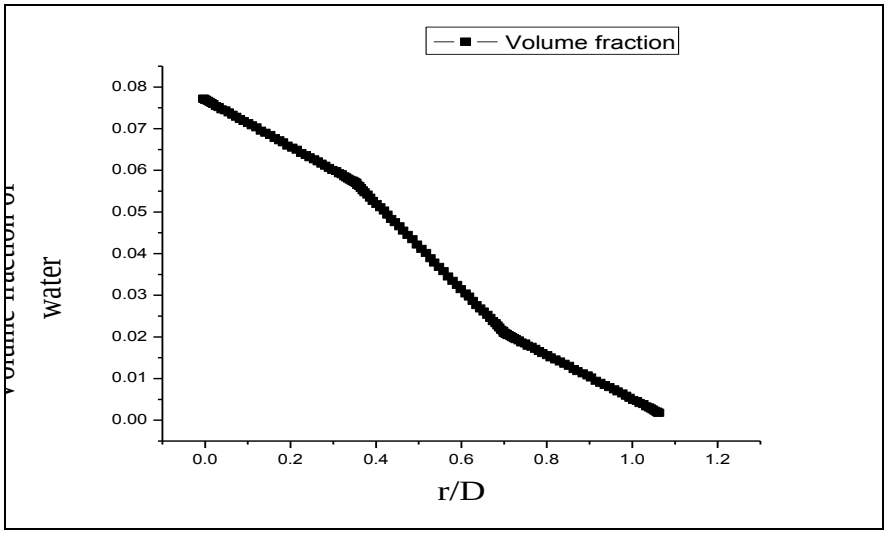

Figure IV.11: *Volume fraction of water.*

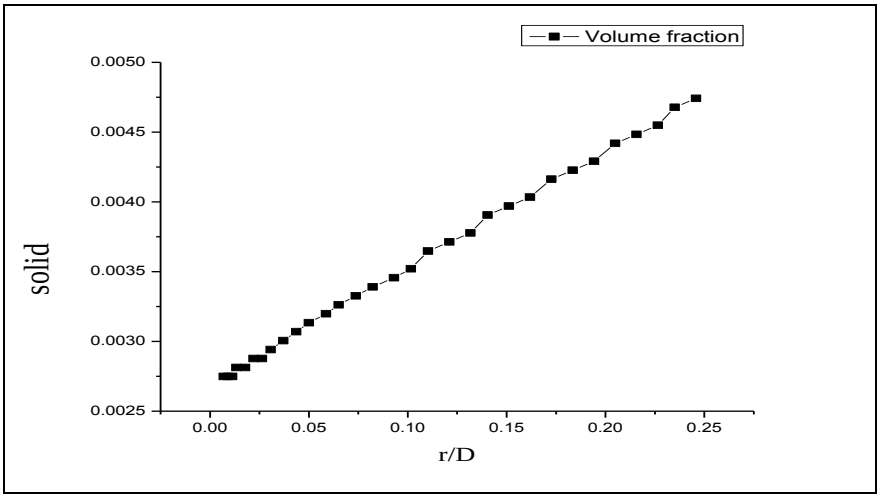

Figure IV.12: *Volume fraction of solid*

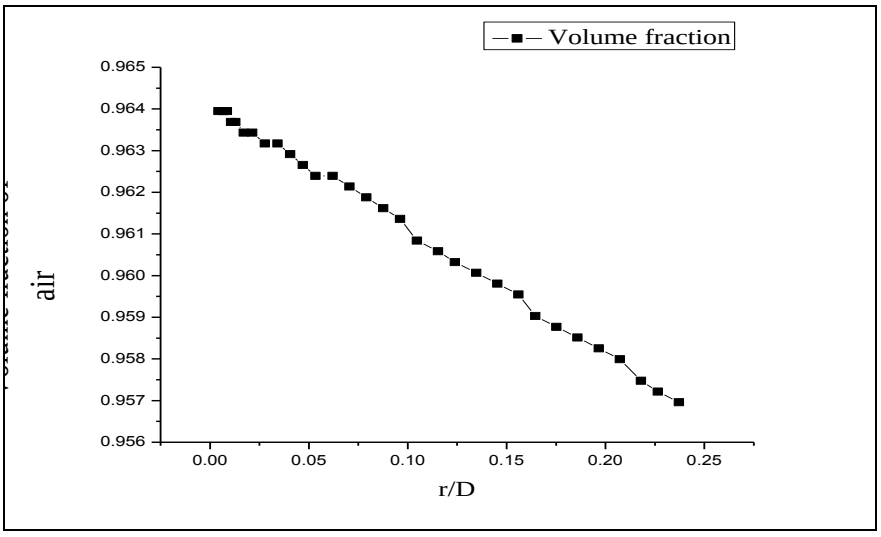

Figure IV.13: *Volume fraction of air.*

IV.5.4. Contour result:

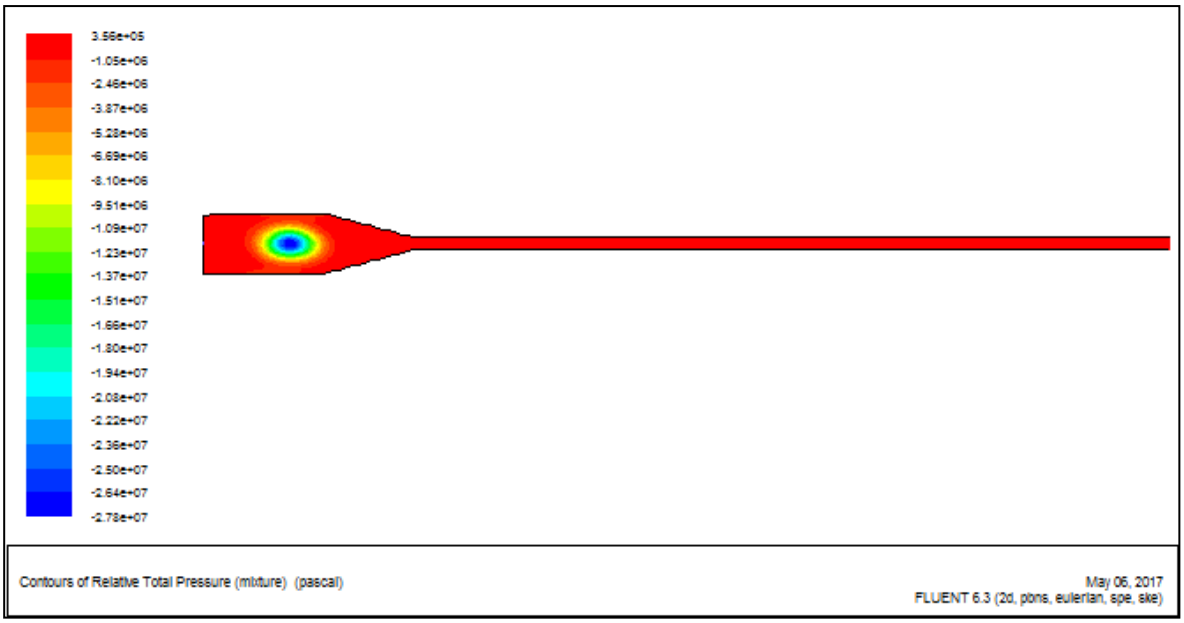

Figure IV.14: *Contour of relative total pressure.*

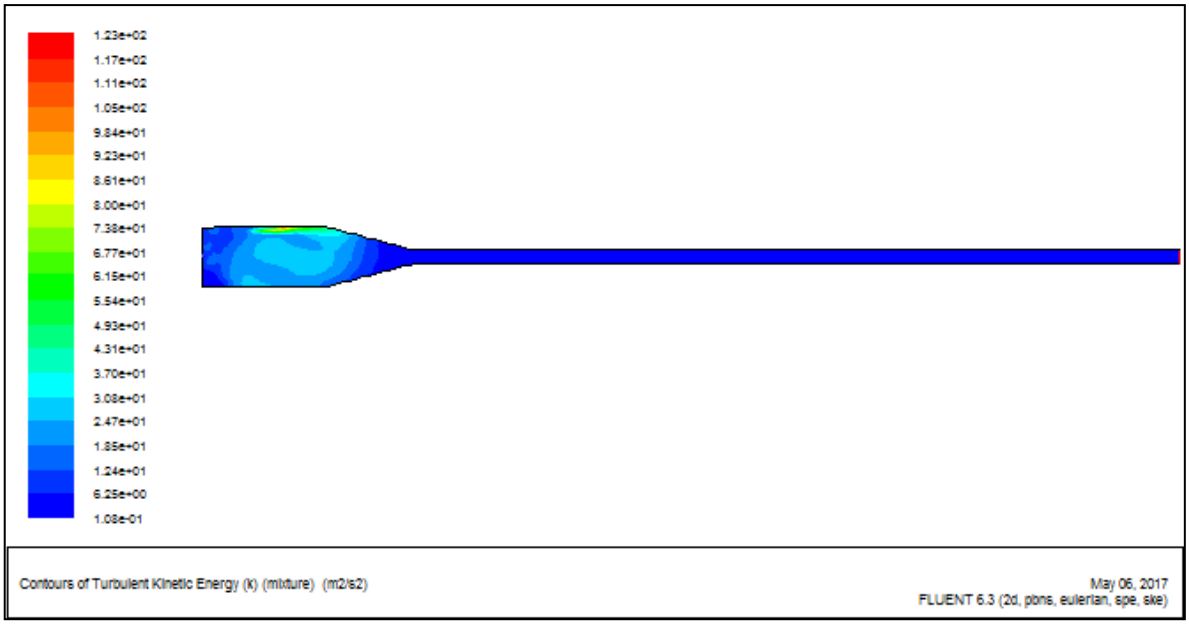

Figure IV.15: *Contour of turbulent kinetic energy.*

The colour scale given to the left of each contours gives the value of the pressure (**figure IV.14**), we can see here the maximum and the minimum of each value and the change that happen in the nozzle. Turbulent kinetic energy in (TKE) is the mean kinetic energy per unit mass association with eddies in turbulent flow; the contour of the kinetic energy has been shown in **figureIV.15**.

IV.5.5. Particle velocity:

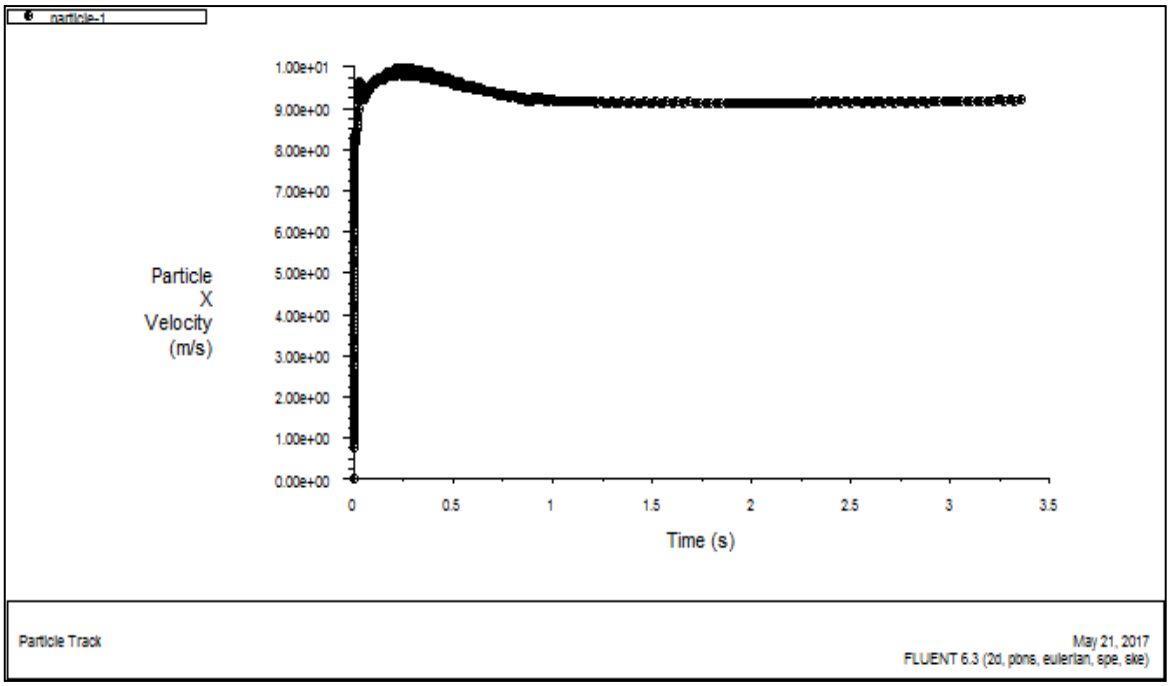

Figure IV.16: *Plot of X velocity of particle.*

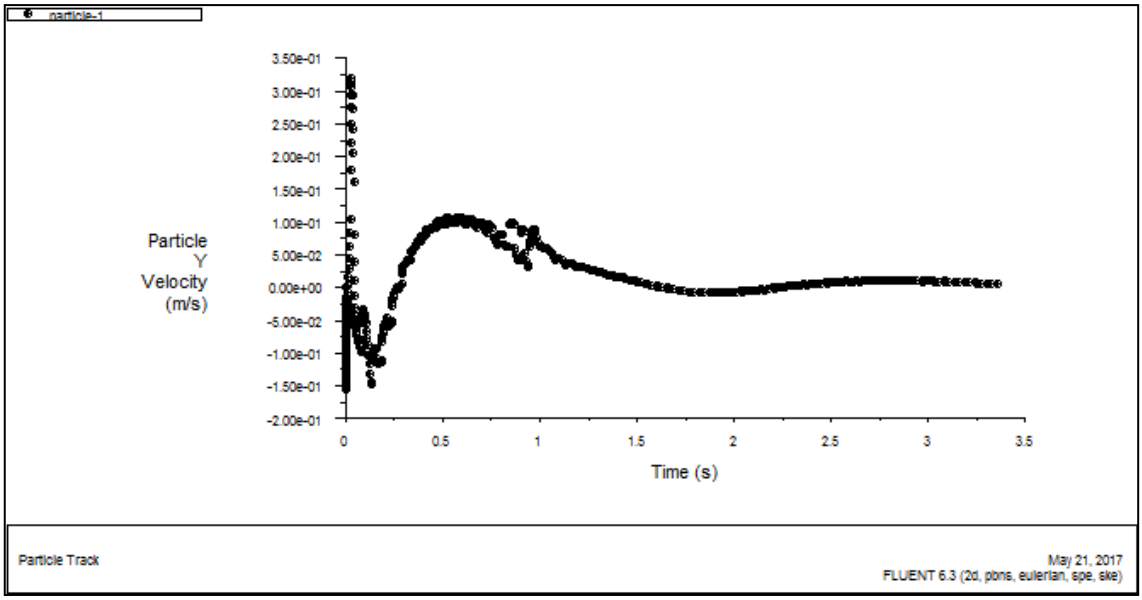

Figure IV.17: *Plot of Y velocity of particle.*

As a result of the convergence, particles are injected from the grit in the flow, the above results are obtained. In the **figures (IV.16)** and **(IV.17)**, a slight decrease of the axial velocity in the first times of the jet since its entry is observed, this follows from a somewhat larger decrease and that The radial velocity increases only until it stabilizes. Since the particles are carried by the fluid, they follow the behavior of the latter.

IV.6. Conclusion:

CFD simulation of three phases has been carried out for different operation by employing the Eulerian-Eulerian approach, Two dimensional numerical simulation has been carried out for different configurations, in three phase flow variables studies included, air, water, solid, the interactions between them was difficult to investigate in experiments so it has been studied numerically, the main conclusion which have been pointed out are:

- The jet velocity at the exit of the focus tube increases with the increase of taper inlet angle for up to 75°;
- Beyond the 75°, the jet velocity start to decrease this may have been due to the length of the taper section that become longer;
- The speed of abrasive is relatively increasing with the increase of taper inlet angle;
- The water increase a lot in 75° inlet may have been due to the particle size or the volume fraction;
- It has been found that the velocity in a smaller diameter of focus tube get to increase compared to the larger diameter:

Finally, our difficulties in obtaining results with the speed of advancement did not prevent us from showing and to have more knowledge on the software FLUENT 6.3.26 and GAMBIT 2.3.16.

CONCLUSION

General conclusion

Abrasive water jet cutting is one of the most recently developed manufacturing technologies; its superiority to many other cutting techniques in processing various materials, this technology is being increasingly used in various industries. However, the velocity distribution in abrasive water jet for precision cutting is very important parameter.

Experimental result for finding the velocity of water and abrasive have been obtained using different methods, but in actual case the abrasive water jet encompasses the flow of three phases (water, air and solid), most of researchers have carried out experimental for the abrasive particles and water since it's difficult to measure the velocity of air at the exit of the focus tube.

The propose of this thesis was to find out the solid, air, water velocity distribution at the outlet of the focus tube, through a numerical simulation based on computational fluid dynamic method. We have found from the simulations that the acceleration process was much better for 75° as taper inlet angle leading to the maximum velocity of the jet at the exit of the focus tube.

In future work and to be able to get a firm conclusion we need a precise mesh size, and more knowledge about the Eulerian model and also some information about the velocity of abrasive and the volume fraction, the result obtained so far are promising but we need a more research for more precise result.

Finally, despite the difficulties that we went through to find the solution and get a reasonable result but it was a real chance for us to get knowledge about numerical simulation and how we use FLUENT software.

REFERENCES

REFERENCES

[1] **Andreas W. Momber, R.Kovacevic**, "*optical method for surface analyses and their utilization for abrasive liquid jet automation*". August 18-21, Minneapolis, Minnesota, (2001).

[2] **Seiji Shimizu**. *"Tribology in Water Jet Processes, New Tribological Ways"*, Dr. Taher Ghrib (Ed.), ISBN: 978-953-307-206-7, InTech, (2011).

[3] **Mohamed Hashish**, "*macro characteristics of AWJ turned surfaces*", Flow International Corporation, Kent, WA, (2001).

[4] **Liu, H., Wang, J., Kelson, N., & Brown, R.J.** "*A study of abrasive water jet characteristics by CFD simulation*". Journal of Material Processing Technology, 153-154, pp. 488-493, (2004).

[5] **Ushata Aish, Asissh Bandyopadhyay, Simul Banerjee, "***A state of the art- review on abrasive water jet machining process"* international review of mechanical engineering (I. RE. M. E)**,** vol. 7, N. 7, ISSN: 19970-8734, November (2013).

[6] **Joseph Giedra,**"*Water Jet Cutter: A Tribological Tool for Various Uses in Industry*", MANE 6963: Friction and Wear of Materials

[7] **Adel. A.Abdel-Rahman, "***An Abrasive Water jet Model for Cutting Ceramics*", Mathematical Models for Engineering Science.

[8] **Giteshkumar N Patel**, *"CFD Simulation of Two-phase and Three-phase Flows in Internal-loop Airlift Reactors*", Master's thesis, Lappeenranta University of Technology, (2010).

[9] **Thome, J.R.** "*Engineering Data Book III",* Wolverine Tube Inc., Alabama, USA, (2004).

[10] **F. Cenac,** " *Etude de l'usinage non débouchant par jet d'eau abrasif des composites*", Ph.D thèses," University Paul Sabatier, (2011).

[11] **J. Munoz, I. Kain, "***abrasive water jet cutting a comparative study between open catcher tank and water catcher tank*", WJTA American Water jet Conference August 18-21, Minneapolis, Minnesota, p166. (2001).

[12] **M. Johnson, D. Burch,R.D. Fossey, D. A. Summers, J. W. Newkirk, G. Galecki,** "*Abrasive cutting comparisons*", WJTA American Water jet Conference August 18-21, . Minneapolis, Minnesota, p144. (2001).

[13] **Z. Yong and R. Kovacevic**.,«*Modeling of jetflow drilling with consideration of the chaotic erosion histories of particles*, ». WEAR, 209, 284-291, (1997).

[14] **Bennacer Latif**., « *Etude et modélisation de la découpe d'un matériau ductile par jet d'eau abrasif.* » PhD thesis, Ecole Nationale Supérieure d'arts et Métiers, centre de Paris, (1998).

[15] **K. R. MomberA.W.,**"*Principles of abrasif water jet machining*". (1998).

[16] **S. Ferrendier**, « *Influence de l'Evolution Granulométrique des Abrasifs sur l'Enlèvement de Matière lors de la découpe par JEA*»Ph.Dthesis, Ecole Nationale Supérieure d'Arts et Métiers, (2001).

[17] **John Olsen and Jiyue Zeng, "***The state-of-the-art of precision abrasive water jet cutting*", Qingdao, China, Oct. 10-12, (2006).

[18] **Chailendra Kumar Pandey**, " *CFD simulation of hydrodynamic of three phase fluidized bed*", Master thesis, May (2010).

[19] **Elin Stenmark, "***On Multiphase Flow Models in ANSYS CFD Softwar",* Master thesis, Chalmers university of technology , Göteborg, Sweden (2013).

[20] **Cristian Birtu1 and ValeriuAvramescu, "***Abrasive water jet cutting technique, equipment, performances",* Nonconventional Technologies Review Romania, March, (2012).

[21] **Hua liu**, "*A study of the cutting performance in abrasive water jet contouring of alumina ceramics and associated jet dynamic characteristics*", PhD thesis, Queensland university of technology, (2004).

[22] **M. Zaki,**«*Modélisation et simulation numérique du procédé de perçage non débouchant par jet d'eau abrasif* », Ph.Dthesis," Ecole Nationale Supérieure d'Arts et Métiers, (2009).

[23] **M. M. Korat, Dr. G. D. Acharya**, "*A Review on Current Research and Development in Abrasive Water jet Machining*", Journal of Engineering Research and Applications, ISSN : 2248-9622, Vol. 4, Issue 1(Version 2), pp.423-432. January (2014).

[24] **Andreas W. Momber and Radovan Kovacevic, "***Principles of Abrasive Water Jet Machining*", Dallas, Texas: Springer-Verlag London Limited 1998, (1997).

[25] **Can Kang, and Haixia Liu**, "*Small-Scale Morphological Features on a Solid Surface Processed by High-Pressure Abrasive Water Jet*", ISSN 1996-1944, 14 August (2013).

[26] **M. Hashish**, "*A model for abrasive water jet machining*", J. Engg. Materials Tech., Vol.111, pp.154-162. (1989).

[27] **A. Bortolussi, R. Ciccu, B. Grosso, "***cutting of reinforced concrete using abrasive suspension jet***",** University of Cagliari, Italy. August 18-21, Minneapolis, Minnesota.p105. (2001).

[28] **Mark Powell,** *"optimization of uhp waterjet cutting heads, the orifice*", Flow International Kent, Washington, August 19-21, Houston, Texas. (2007).

[29] **Thomas Kuriakose,** *"A Study of Annular Slurry Jet for Abrasive Water jet Cutting"*, Master thesis, New Jersey Institute of Technology, October, (1992).

[30] **Abou-el-foutouhtazibt,** *" Etude théorique et expérimentale du processus d'accélération de particules abrasives dans un jet d'eau sous très haute pression*", PhD theses, L'Université des Sciences et Technologies de Lille, Janvier (1995).

[31] **R.T. Deam, E. Lemma, and D.H. Ahmed**., "*Modeling of the abrasive water jet cutting process*", WEAR, 257, pp. 877-891, (2004).

[32] **F. Moukalled, L. Mangani, M. Darwish**, "*the finite volume method in computational fluid dynamic"*, Institute of Engineering Thermodynamics, Stuttgart, Germany, vol.113.pp. 4-5.

[33] **Guide gambit**, Fluent (1998–2007).

[34] **Dewan H. Ahmed, Elias Siores, Jamal Naser, Frank L. Chen,***" Numerical Simulation of Abrasive Water Jet for Different Taper Inlet Angles*", University Adelaide, Australia, December (2001).

[35] **Zoltani, C. K., and Bicen, A. F**., *"Velocity Measurement in a Turbulent*", Dilute, Two-phase Jet," Experiments in Fluids, Vol. 9, 1990, pp. 295-300.

[36] **Ye, J**, *"Numerical Simulation of Particle Concentration at the Exit of a Direct Injected Abrasive Water Jet Nozzle"*, Particulate Science and Technology, Vol. 14, 1996, pp.75-88.

[37] **V.K. Jain**, " advanced machining process", Allied publicher, private limited, india. (2002).

[38] **Z.Guo, M.Rannulu,** " *analysis of the wate rjet contact impact on target material, optic and laser in engineering*", Vol.33, N02. Pp121-139. (2000).

[39] **A.I. Hassan, J. Kosmal, "***dynamic elastic-plastic analysis of 3D deformation in AWJM*", journal of materials processing technology. Vol.153-154, pp488-493. (2004).

[40] **M.Junkar, B.Jurisavic, "** *finit element analysis of single particule impact in AWJM***",** International journal of impact engineering. Vol 32. Pp1095-1112.(2006).

[41] **Y.F.Wang, Z.G, Young, "** *finit element model of erosive wear on ductile and brittle materials processing technology*", Vol 209, n.9, pp 4573-4577.(2009).

[42] **J.Wang, "***particle velocity model for ultra-high pressure AWJ***",** journal of material processing technology. Vol 209, n9, pp 4573-4577.(2009).

[43] **M.Takaffoli, M.papini, "***finite element analysis of single impact of angular particles on ductile target wear*", Vol 267, n1-4,pp 144-151.2009.

[44] **MA. AZ.mir, AK.Ahsan**, "investigation *on glass lepoxy composite surface machined by AWJM*", journal of materials processing technology, Vol.198, n1-3, pp122-128.(2003).

[45] **J. Wang**, "*abrasive WJM of polymer matrix composites-cutting performance*", international journal advanced manufacturing technology, Vol.15, n10, pp757-768.

Abstract:

A computational fluid dynamics (CFD) method has been developed to find out the particle and air, water velocity at the exit of the focus tube, the study has been carried out using a multi-phase approach, the abrasive particle were treated as a solid granular continuous phase, the air used for pumping the abrasive particles into the jet device was treated as a continuous phase and the water as a principle continuous phase. The governing equation were discretized using the finite volume approach, the solution was obtained using Euleurian model. The results clearly shows the effect of the taper inlet angles on the velocity of water, abrasive, air at the exit of the focus tube, and were compared with the experimental data.

Keywords: CFD, Euleurian, abrasive, velocity, turbulent model, taper inlet angle, multi-phase.

Résume:

Une méthode de calcul de la dynamique des fluides (CFD) a été développée pour découvrir la vitesse de l'air et de l'eau à la sortie du tube de focalisation, l'étude a été réalisée en utilisant une approche multi-phase, la particule abrasive a été traitée comme un solide Phase continue granulaire, l'air utilisé pour pomper les particules abrasives dans le dispositif à jet a été traité comme une phase continue et l'eau comme phase continue principale. L'équation de régulation a été discrétisée en utilisant l'approche du volume fini, la solution a été obtenue en utilisant le modèle Euleurian. La simulation a été effectuée en utilisant différents angles d'entrée coniques, les résultats montrent clairement l'effet des angles d'entrée coniques sur la vitesse à la sortie du tube de focalisation et ont été compares aux données expérimentales.

Mot clés: CFD, particules abrasive, Euleurian, turbulent, multi-phase, vitesse, angle d'entrée conique

التلخيص:

قد تم تطوير طريقة ديناميكية السوائل الحسابية (د.س.ح) لمعرفة الجسيمات والهواء وتوزيع المياه عند خروج أنبوب التركيز، وقد أجريت الدراسة باستخدام نهج متعدد المراحل، وتم التعامل مع الجسيمات الصلبة كمرحلة مستمرة، تم معاملة الهواء المستخدم لضخ الجسيمات الصلبة في الجهاز كمرحلة مستمرة والماء كمرحلة ابتدائية مستمرة. الحصول على الحل باستخدام نموذج يوليوريان .أجريت المحاكاة باستخدام زوايا مدخل مختلفة، والنتائج تظهر بوضوح تأثير زوايا مدخل على سرعة الماء، الجسيمات الصلبة، الهواء عند خروج أنبوب التركيز، وتمت مقارنتها مع البيانات التجريبية الموجودة في المرجع.

الكلمات المفتاحية: ديناميكية السوائل الحسابية،الجسيمات الصلبة،يوليوريان،كاي-ابلسيلون، السرعة، زوايا المدخل، متعدد المراحل.